# Integrating Reconfigurable Intelligent Surface and UAV for Enhanced Secure Transmissions in IoT-Enabled RSMA Networks

Dawei Wang, Jiawei Li, Qinyi Lv, Yixin He, Li Li,
Qiaozhi Hua, Osama Alfarraj, and Jiankang Zhang

***Abstract*—Unmanned aerial vehicle (UAV)-enabled Internet of Things (IoT) exhibits great application potential with its wide coverage, flexible network topology, and diversified services. However, ensuring communication security and efficient spectrum resource utilization in multi-user access scenarios is challenging, given the open nature of UAV channels and the proliferation of communication devices in IoT. To address the above challenges, this paper proposes a novel reconfigurable intelligent surface (RIS)-aided UAV collaborative communication framework, where RIS-equipped UAV flexibly serves multiple users. In this work, a rate splitting multiple access (RSMA)-based secure transmission scheme is proposed, where the split public information serves both as useful signals and noise to disrupt eavesdropping. For the proposed scheme, a sum secrecy rate maximization problem is formulated and solved by optimally deploying the UAV's location, designing the RIS's phase shift, and power allocation. For this non-convex problem with a couple of variables, we decompose it and form three separate sub-issues. Specifically, leveraging the successive convex approximation (SCA) and semidefinite relaxation (SDR) techniques, we first exploit an iterative algorithm for optimizing beamforming vectors and phase-shift matrix of RIS, and the optimal position of the UAV is obtained according to the deep deterministic policy gradient (DDPG). Then, we design an alternating optimization (AO) framework for joint solving. Finally, simulation results validate the efficacy of the proposed scheme in enhancing security, e.g., relative to the non-orthogonal multiple access (NOMA) scheme and benchmark scheme, the secrecy rate of the proposed scheme increased by 29.7% and 71.9% respectively.**

***Index Terms*—Internet of Things, unmanned aerial vehicle, reconfigurable intelligent surface, rate splitting multiple access, security.**

This work was supported in part by the National Natural Science Foundation of China under Grant 62271399, Grant 62401230, Grant 62301434, and Grant 62201462, in part by National Key Research and Development Program of China under Grant 2024YFC2206804, in part by the Foundation of the Science, Technology, and Innovation Commission of Shenzhen Municipality under Grant JCYJ20190806160218174, in part by the Practice and Innovation Funds for Graduate Students of Northwestern Polytechnical University under Grant PF2024009, and in part by the Researchers Supporting Project Number (RSP2024R102), King Saud University, Riyadh, Saudi Arabia. *(Corresponding author: Qiaozhi Hua).*

Dawei Wang, Jiawei Li, Qinyi Lv, and Li Li are with the School of Electronics and Information, Northwestern Polytechnical University, Xi'an, Shaanxi, 710072, China, and also with the Research & Development Institute of Northwestern Polytechnical University in Shenzhen, Shenzhen, Guangdong, 518057, China. (e-mail: wangdw@nwpu.edu.cn; lijw@mail.nwpu.edu.cn; lvqinyi@nwpu.edu.cn; lil@nwpu.edu.cn).

Yixin He is with the College of Information Science and Engineering, Jiaxing University, Jiaxing 314001, China, and also with the Jiaxing Key Laboratory of Smart Transportations, Jiaxing 314001, China. (e-mail: yixinhe@zjxu.edu.cn).

Qiaozhi Hua is with the Computer School, Hubei University of Arts and Science, Xiangyang 441000, China. (11722@hbuas.edu.cn)

Osama Alfarraj is with the Computer Science Department, Community College, King Saud University, Riyadh 11437, Saudi Arabia. (e-mail: oalfarraj@ksu.edu.sa).

Jiankang Zhang is with the Department of Computing and Informatics, Bournemouth University, BH12 5BB Poole, U.K. (e-mail: jzhang3@bournemouth.ac.uk).

## I. Introduction

### A. Background

The Internet of Things (IoT), which consists of the Internet, sensor networks, and traditional telecommunications networks, is an important support for the next generation of communication technology. Facing the urgent requirements for efficient and seamless coverage, unmanned aerial vehicle (UAV)-enabled IoT, having the advantages of cost-effective, high throughput, and flexible network architecture, have attracted widespread attention [1]. With high mobility and convenient deployment, UAVs can achieve efficient data transmission and comprehensive communication coverage as aerial relays and have been widely used in emergency rescue, intelligent transportation, and other fields [2]. However, UAVs face power limitations when forwarding information, and in complex urban scenarios, the air-to-ground channels are susceptible to interference from buildings or environmental fading, resulting in degraded channel quality. Reconfigurable intelligent surface (RIS), composed of low-cost electromagnetic materials, offers a solution by reconfiguring channels through beamforming and parameter adjustments, thereby effectively enhancing backscatter communications and solving the above problems. Compared with traditional networks where RIS is fixed on the surface of buildings, UAV-RIS communication networks leverage flexible mobility and channel improvement capabilities and have superiority in improving communication performance such as throughput and energy efficiency [3].

In the UAV-RIS network, the connection between the UAV and ground devices is typically not obstructed and relies on line-of-sight transmission. The wireless channel exhibits broadcast characteristics, making information susceptible to eavesdropping. Therefore, how to reduce information leakage and ensure communication security is an important challenge. Physical layer security (PLS) exploits the randomness and diversity of legitimate transceivers to ensure information security with less complexity compared to conventional encryption methods [4], [5]. Utilizing PLS encryption technology, UAV-RIS-assisted communication can further improve secrecy performance. Aerial RIS boosts the strength of legitimate signals

by adjusting its phase, while simultaneously degrading the quality of the eavesdropping channel to prevent eavesdropping. Moreover, the agile mobility of UAVs enables them to evade potential eavesdroppers, thereby enhancing secrecy performance to a certain degree.

As the IoT rises and the proliferation of communication equipment, current communication networks face the challenges of limited multi-user spectrum resources. To improve the utilization of communication resources, Non-orthogonal multiple-access (NOMA) technology realizes multi-user access by exploiting channel quality differences for time and spectrum resource allocation, and successive interference cancellation (SIC) is applied to resolve interference [6]. Despite its advantages, NOMA requires multiple SIC processes at the receiving end, which leads to increased decoding complexity and the need for decoding order optimization. In contrast, the more flexible rate splitting multiple access (RSMA) technology has garnered significant interest from researchers. RSMA segregates information and consolidates all common information into a unified information stream, thus receivers only need to use SIC once. Furthermore, RSMA eliminates the need for decoding order optimization, reducing decoding complexity and addressing the issue of limited spectrum resources for multiple users. Current researches indicate that RSMA offers greater advantages than NOMA and space division multiple access (SDMA) technologies in enhancing communication efficiency [7].

### *B. Related Works*

In intricate communication scenarios, the direct connection from the base station to the ground users often face disruptions caused by building obstructions, while environmental fading further affects communication performance. Leveraging the agile mobility of UAVs and the channel optimization capabilities of RIS, the RIS-UAV communication architecture emerges as a promising solution to the above problems [8], [9]. In [10], the application of RIS in satellite communications was explored, the authors investigated the effect of RIS parameters on performance improvement by deriving equations for outage probability and signal-to-noise ratio. The authors in [11] proposed a multi-RIS-assisted downlink UAV communication network, where multiple RIS are installed on the surface of buildings to provide communication services to ground users with a single antenna through UAV movement. The RIS selection strategy was analyzed under two conditions, outdated and incomplete channel state information. The authors in [12] designed a comprehensive optimization algorithm for multi-UAV joint task offloading and edge computing problems, integrating path planning and joint scheduling to facilitate real-time communication service transmission while minimizing system energy consumption. In addition, compared with the scheme of fixed RIS location, existing studies have shown that mobile RIS communication has significant advantages, especially in reducing energy consumption and maximizing throughput [13], [14].

Considering the communication security issues caused by information leakage, PLS utilizes the uniqueness and time variability of wireless channels and has gained researchers' favor in the green communications field. Currently, RIS is being extensively explored as a potent augmentation to PLS. In [15], the authors delved into RIS-assisted uplink three-dimensional heterogeneous networks and evaluated the secrecy performance by analyzing channel fading and closed-form expressions for signal-to-noise ratio. To enhance secrecy performance, in [16], the authors proposed a two-way training scheme to detect active eavesdropping scenarios, and transmit beamforming and RIS phase shift were jointly optimized for maximizing security rate. To address the two security threats of active interference and passive eavesdropping in the uplink communication link, the authors in [17] proposed a scheme to maximize the average secrecy rate by optimizing the transmit power, RIS phase shift, and UAV trajectory. Moreover, UAV-RIS can also be used as an air edge server. In scenarios with potential eavesdroppers, RIS was employed to offload computing tasks to the base station, then the authors jointly considered the three variables, the UAV trajectory, RIS beamforming, and computing task assignment, to ensure secure computing for users [18].

Although the aforementioned research has demonstrated the superiority of UAV-RIS networks, as the number of communication devices continues to surge, the challenge of effectively utilizing spectrum resources has become a focal point in academic research. RSMA emerges as a flexible and robust multiple-access technology. In the RSMA system, deep learning [19] and SCA algorithms [20], [21] can be utilized for power control and channel allocation, thereby striking a balance between spectrum efficiency and energy consumption. Furthermore, RIS-assisted RSMA networks have exhibited enhanced communication performance. In [22], to improve the weighted sum rate, the authors employed UAV-RIS as a full-duplex relay to serve multiple users and devised a heuristic algorithm based on block coordinate descent technology. In [23] and [24], the authors respectively proposed an alternating optimization framework and a LogSumExp method to transform the non-convex confidentiality problem into a convex problem, thereby improving the confidentiality performance of the downlink RSMA network. The simulation results proved the superiority of the RSMA strategy. However, in both schemes, the RIS position is fixed, and the impact of dynamic adjustment of the RIS position on system performance is not considered. Optimizing the RIS position can further improve channel quality and network security, especially in multi-user scenarios. Therefore, future research could explore the integration of RIS position optimization with RSMA strategy to enhance overall communication performance and security.

### *C. Motivations and Contributions*

Although existing works have investigated UAV-RIS cooperative communication and RSMA-based multi-user networks, some technical issues remain under-addressed. First, in RSMA communication networks, existing studies [20]–[22] have extensively explored performance enhancements in spectrum utilization, system throughput, and energy efficiency. However, the information security of RSMA systems has

not been sufficiently considered. Attacks and eavesdropping by eavesdroppers in the network can lead to data leakage and communication interruptions, posing serious privacy risks and potential economic losses for users. Therefore, an urgent need is to study effective security enhancement schemes for RSMA systems to protect data information and ensure communication reliability. Second, in RIS-assisted UAV communication scenarios, the potential advantages of RSMA for multi-user communication have not been comprehensively studied. In [10]–[16], RIS served multiple users as an aerial relay, but the problem of limited spectrum resources in multi-user communication scenarios is overlooked, which can cause interference between multiple users and lead to a decrease in communication quality. Regarding information security concerns, [23] and [24] effectively utilized the technical advantages of RIS and RSMA and adopted PLS technology to reduce the quality of the eavesdropping channel to ensure communication security. However, the authors fixed the UAV position for auxiliary communication without considering the potential benefits of the UAV's mobility.

Inspired by the preceding discussion, we propose a novel RIS-assisted UAV-RSMA cooperative communication framework, where the UAV carrying RIS provides communication services to multiple users through positional adjustments. In addition, RSMA technology is introduced to solve the problems of interference between multiple users and limited spectrum resources, achieving information security while improving spectrum efficiency. The main contributions of this paper are summarized as follows.

- Firstly, considering the secure communication of UAV-RIS, a novel communication framework is proposed. In this framework, UAV serves as an aerial relay for information forwarding and the RSMA technology is incorporated to enhance multi-user spectrum efficiency. Additionally, for the eavesdropper existing in the network, precoding public information is utilized as noise to effectively deter eavesdropping. To ensure information security, we propose a secure transmission optimization scheme aimed at maximizing the sum secrecy rate of the network.
- Secondly, given that three optimization variables: the beamforming vectors, RIS phase shift matrix, and UAV position are highly interrelated, we decouple the optimization problem. Specifically, we employ SCA and SDR techniques to solve for the beamforming vectors and RIS phase shift matrix optimization respectively, followed by the use of an iterative algorithm for joint optimization. The optimal UAV position is established using the DDPG algorithm. On this basis, an alternating optimization algorithm is devised to execute a joint optimization solution, and complexity analysis is conducted.
- Finally, we validate the secrecy performance of the proposed sum secrecy rate maximization scheme through numerous simulations. The simulation results demonstrate that the sum secrecy rate is enhanced by 29.7% and 71.9% compared to the security solution based on the NOMA technology [29] and the benchmark scheme employing random phase shifts of RIS. Furthermore, we analyze the impact of system parameters on secrecy performance, such as the base station's maximum transmit power, number of RIS reflective elements, and number of transmit antennas.

### D. Organization

The subsequent sections of this paper are outlined as follows. Section II introduces the communication and channel modeling of the UAV-RSMA network and the sum secrecy rate maximization problem is proposed. In Section III, we give the detailed solution process of the three sub-problems of SCA, SDR, and DDPG algorithms, and propose an alternating iterative optimization framework. Section IV is the simulation parameters and experimental results of this paper. Section V is the conclusion.

## II. System Model and Problem Formulation

### A. Downlink Dual-User RSMA Communication Model

Figure 1 illustrates a RIS-assisted downlink UAV-RSMA collaborative communication framework, which comprises a source base station (SBS) equipped with $K$ transmitting antennas, a UAV deployed with RIS as an aerial relay to serve the terrestrial users, and an eavesdropper (Eve) exists in the system to steal the classified information. Due to the obstruction of high buildings on the ground or the effect of environmental fading, the direct communication link between SBS and ground users is interrupted. Therefore, the UAV carrying RIS is used as an air relay to ensure normal communication between the SBS and ground users.

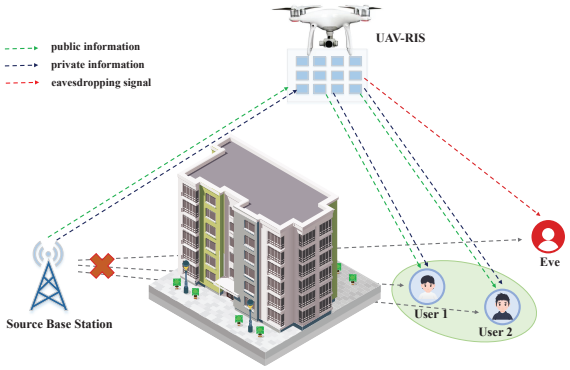


Fig. 1. A RIS-assisted downlink UAV-RSMA collaborative communication framework.

The communication process consists of two hops: the SBS first sends the information to the UAV, and the UAV forwards the information to the ground user. The locations of the SBS and two ground users in the coordinate system can be represented respectively as $\mathbf{L_s} = [x_s, y_s]$, $\mathbf{L_1} = [x_1, y_1]$ and $\mathbf{L_2} = [x_2, y_2]$. Numerous research works focus on communication sensing and radar positioning [30], [31]. Consequently, the eavesdropper's location $\mathbf{L_e} = [x_e, y_e]$ can be inferred from these studies. The UAV flying time contains $N$ time slots, and the UAV position can be considered constant for

each time slot when $N$ is large enough, and the UAV position is $\mathbf{L}[\mathbf{n}] = [x[n], y[n]]$, $n \in \forall N$. The height of the UAV is $H_u$. RIS has $M$ reflective elements and the phase matrix is $\mathbf{\Theta} = diag(e^{i\varphi_1}, e^{j\varphi_2}, ..., e^{j\varphi_M}) \in \mathbb{C}^{M\times M}$, where $\varphi_i \in [0, 2\pi), i \in \{1, 2, ..., M\}$ denotes the $i$-th reflection element's phase shift.

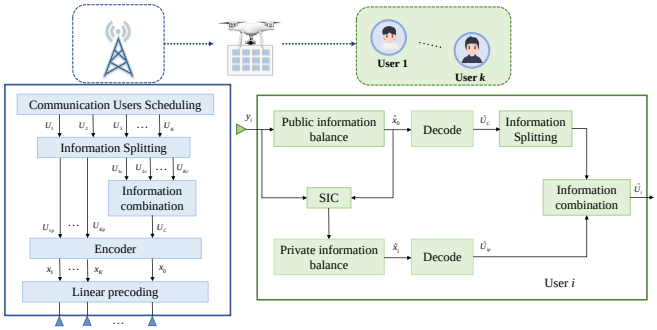


Fig. 2. The RSMA technical framework.

The RSMA strategy is adopted to serve multiple users and the RSMA technical framework is shown in Fig. 2. In the downlink RSMA communication network, the SBS first linearly precedes the information through the precoder. Referring to the one-layer RS model, the SBS divides the sent information into public information $I_0$ and each user's private information $I_{p,1}$, $I_{p,2}$. Since public information contains non-private information for all users, all users need to decode the public information first and then decode the private information sent to them. The transmit signal of SBS is defined as

$$\mathbf{x} = \boldsymbol{\omega}_0 x_0 + \sum_{k=1}^{2} \boldsymbol{\omega}_k x_k = \boldsymbol{\omega}_0 x_0 + \boldsymbol{\omega}_1 x_1 + \boldsymbol{\omega}_2 x_2, \quad (1)$$

where $x_0$, $x_1$, $x_2$ are public information and private information of two users, and $\mathbf{x} \in \mathbb{C}^{K\times 1}$. $\boldsymbol{\omega}_0$, $\boldsymbol{\omega}_1$ and $\boldsymbol{\omega}_2$ are the beamforming vectors of public information and private information sent to user 1 and user 2, and $\boldsymbol{\omega}_0, \boldsymbol{\omega}_1, \boldsymbol{\omega}_2 \in \mathbb{C}^{K\times 1}$. Information streams $x_0$, $x_1$, $x_2$ are independent of each other and carry only a unit of energy, i.e., $E\left\{\|x_0\|^2\right\} = E\left\{\|x_1\|^2\right\} = E\left\{\|x_2\|^2\right\} = 1$.

The signals received by ground user 1 and user 2 can be represented as

$$y_1 = \mathbf{h}_1\mathbf{x} + n_1 = \mathbf{h}_{r,1}^H \mathbf{\Theta} \mathbf{H}_{\text{SR}} (\boldsymbol{\omega}_0 x_0 + \sum_{k=1}^{2} \boldsymbol{\omega}_k x_k) + n_1, \quad (2)$$

$$y_2 = \mathbf{h}_2\mathbf{x} + n_2 = \mathbf{h}_{r,2}^H \mathbf{\Theta} \mathbf{H}_{\text{SR}} (\boldsymbol{\omega}_0 x_0 + \sum_{k=1}^{2} \boldsymbol{\omega}_k x_k) + n_2. \quad (3)$$

Since the SBS is far away from the ground users and it may be blocked by tall buildings, the direct link between the SBS and users is absent. Thus, the communication channel from SBS to users can be stated as

$$\mathbf{h}_k = \mathbf{h}_{r,k}^{\text{H}} \mathbf{\Theta} \mathbf{H}_{s_R}, k \in \{1, 2, e\}, \quad (4)$$

where $\mathbf{h}_k \in \mathbb{C}^{1\times K}$. $\mathbf{h}_{r,k}$ and $\mathbf{H}_{\text{SR}}$ denote the RIS-users and SBS-RIS communication channels.

In particular, the SBS is outfitted with $K$ transmitting antennas, employing uniform linear array (ULA). Therefore, the channel from SBS to UAV-RIS for the first hop can be expressed as

$$\mathbf{H}_{\text{SR}} = \sqrt{\beta_0 d_{rs}^{-\alpha}} \mathbf{a}_R(\theta, \phi) \mathbf{a}_s^T(\theta) \in \mathbb{C}^{M\times K}, \quad (5)$$

where $\beta_0$ denotes the channel gain at $d = 1m$, $\alpha$ represents the air-to-ground path loss, and $d_{sr}$ is the distance from SBS to UAV, denoted as $d_{sr} = \sqrt{(\mathbf{L}[n] - \mathbf{L}[s])^2 + H_u^2}$. $\mathbf{a}_s$ is the array steering vector of the SBS equipped with $K$ transmitting antenna, which can be denoted as

$$\mathbf{a}_s(\theta) = \left[1, e^{j\frac{2\pi d}{\lambda}\sin\theta}, e^{j\frac{2\pi d}{\lambda}(K-1)\sin\theta}\right]^T \in \mathbb{C}^{K\times 1}, \quad (6)$$

where $d$ and $\lambda$ represent the distance and wavelength between adjacent antennas respectively, and satisfy $d = \lambda/2$. $d_{sr}^h[n]$ is the two-dimensional horizontal distance from the SBS to the RIS, and the sine of the angle of deviation of the signal at the SBS is defined as $\sin\theta = \frac{d_{sr}^h[n]}{d_{sr}[n]}$. The RIS is in the $yoz$ plane and its $M$ reflective elements are arranged in a rectangular shape, and adopt a uniform linear array (UPA). Then the antenna array response of the RIS is expressed as

$$\mathbf{a}_R(\theta, \phi) = \left[1, \ldots, e^{j\frac{2\pi d}{\lambda}(M_y-1)\sin\theta\sin\phi}\right]^T \otimes \left[1, \ldots, e^{j\frac{2\pi d}{\lambda}(M_z-1)\cos\theta}\right]^T \in \mathbb{C}^{M\times 1}, \quad (7)$$

where $M = M_y M_z$, and $\theta$ represents the residual angle from RIS to $z$-axis positive, known as the elevation angle. $\phi$ is the azimuth angle, which is the angle between the position of the RIS projected onto the $xoy$ plane and the positive direction of the $x$-axis, and $\cos\theta = \frac{H_u}{d_{sr}[n]}$, $\sin\theta\sin\phi = \frac{y_s - y[n]}{d_{sr}[n]}$.

For second-hop communication, the signal received by the UAV is forwarded to the ground users through RIS reflection. Given the maturity of channel estimation technology in the RIS networks [13]–[16], the RIS-user channel can be modelled as the classic Rician fadingwe. The communication includes line-of-sight (LoS) transmission and non-line-of-sight (NLoS) transmission. Ground users and eavesdropper are fitted with single antenna, so the channel between RIS and ground users and eavesdropper can be expressed as

$$\mathbf{h}_{r,k} = \sqrt{\beta_0 d_{rk}^{-\alpha}} \left(A \cdot \mathbf{h}_k^{LoS} + B \cdot \mathbf{h}_k^{\text{NLoS}}\right) \in \mathbb{C}^{M\times 1}, \quad (8)$$

where $\cos\theta = \frac{H_u}{d_{rk}[n]}$, $\sin\theta\sin\phi = \frac{y_k - y[n]}{d_{rk}[n]}$, $k \in \{1, 2, e\}$, and

$$\begin{cases} A = \sqrt{\frac{K_u}{K_u+1}}, B = \sqrt{\frac{1}{K_u+1}}, \\ \mathbf{h}_k^{LoS} = \left[1, \ldots, e^{j\frac{2\pi d}{\lambda}(M_y-1)\sin\theta\sin\phi}\right]^T \\ \qquad\qquad \otimes \left[1, \ldots, e^{j\frac{2\pi d}{\lambda}(M_z-1)\cos\theta}\right]^T, \end{cases} \quad (9)$$

where $K_u$ denotes the Rice factor, and $d_{rk} = \sqrt{(\mathbf{L}[n] - \mathbf{L}_k)^2 + H_n^2}$ is the distance between the RIS and the ground users, the eavesdropper. $\mathbf{h}_\kappa^{LoS} \in \mathbb{C}^{M\times 1}$ is the LoS component, and $\mathbf{h}_\kappa^{NLoS} \in \mathbb{C}^{M\times 1}$ represents the NLoS

channel random scattering component that obeys a complex Gaussian distribution, i.e., $\mathbf{h}_k^{NLas} \sim \mathcal{CN}(0,1)$.

Similarly, the received signal of the eavesdropper can be denoted as

$$y_e = \mathbf{h}_e\mathbf{x} + n_e = \mathbf{h}_{r,e}^H \boldsymbol{\Theta}\mathbf{H}_{\mathrm{SR}}(\boldsymbol{\omega}_0 x_0 + \sum_{k=1}^{2}\boldsymbol{\omega}_k x_k) + n_e, \quad (10)$$

where $n_i\,(i \in \{1,2,e\})$ is the additive white Gaussian noise (AWGN), following $n_i \sim \mathcal{CN}(0, {\sigma_n}^2)$.

According to the RSMA decoding principle, when the ground user receives information, the ground user first needs to decode the public information. During this process, the users' private information are regarded as interference. Therefore, the SINR for decoding the public information are stated as

$$\gamma_{c,1} = \frac{\left|\mathbf{h}_{r,1}^H \boldsymbol{\Theta}\mathbf{H}_{\mathrm{SR}} \cdot \boldsymbol{\omega}_0\right|^2}{\left|\mathbf{h}_{r,1}^H \boldsymbol{\Theta}\mathbf{H}_{\mathrm{SR}} \cdot \boldsymbol{\omega}_1\right|^2 + \left|\mathbf{h}_{r,1}^H \boldsymbol{\Theta}\mathbf{H}_{\mathrm{SR}} \cdot \boldsymbol{\omega}_2\right|^2 + \sigma_1^2}, \quad (11a)$$

$$\gamma_{c,2} = \frac{\left|\mathbf{h}_{r,2}^H \boldsymbol{\Theta}\mathbf{H}_{\mathrm{SR}} \cdot \boldsymbol{\omega}_0\right|^2}{\left|\mathbf{h}_{r,2}^H \boldsymbol{\Theta}\mathbf{H}_{\mathrm{SR}} \cdot \boldsymbol{\omega}_1\right|^2 + \left|\mathbf{h}_{r,2}^H \boldsymbol{\Theta}\mathbf{H}_{\mathrm{SR}} \cdot \boldsymbol{\omega}_2\right|^2 + \sigma_2^2}, \quad (11b)$$

where ${\sigma_1}^2 = {\sigma_2}^2 = \sigma^2$. According to Shannon's formula, the information rate at which user 1 and user 2 decode common information is $R_{c,1} = B\log_2(1+\gamma_{c,1})$ and $R_{c,2} = B\log_2(1+\gamma_{c,2})$, respectively. However, in order to ensure that public information $I_0$ is obtained successfully and decoded by ground users, the public information rate ought not to exceed $R_c = \min\{R_{c,1}, R_{c,2}\}$ during actual transmission. The public information rate of ground users should satisfy $\sum_{k=1}^{2} {r_c}^k \le R_c$, where ${r_c}^k$ is the public information rate allocated by user $k$.

Then, the ground users use the SIC technique to decode the public information and then remove the decoded public information, and then start to decode the private information sent by the SBS, while regarding the private information of the other user as interference. So the SINR for user 1 and user 2 decoding their own private information can be denoted as

$$\gamma_{p,1} = \frac{\left|\mathbf{h}_{r,1}^H \boldsymbol{\Theta}\mathbf{H}_{SR} \cdot \boldsymbol{\omega}_1\right|^2}{\left|\mathbf{h}_{r,1}^H \boldsymbol{\Theta}\mathbf{H}_{SR} \cdot \boldsymbol{\omega}_2\right|^2 + \sigma^2}, \quad (12a)$$

$$\gamma_{p,2} = \frac{\left|\mathbf{h}_{r,2}^H \boldsymbol{\Theta}\mathbf{H}_{SR} \cdot \boldsymbol{\omega}_2\right|^2}{\left|\mathbf{h}_{r,2}^H \boldsymbol{\Theta}\mathbf{H}_{SR} \cdot \boldsymbol{\omega}_1\right|^2 + \sigma^2}. \quad (12b)$$

Therefore, the information rates for ground users are $R_{p,1} = B\log_2(1+\gamma_{p,1})$ and $R_{p,2} = B\log_2(1+\gamma_{p,2})$.

For the sake of generality, private information generally exists in the private information stream sent to each user. Since the base station first pre-encodes the information before it is sent, the public information stream is used as noise to interfere with eavesdropping when the eavesdropper eavesdrops on the private information of each user. Therefore, the information rate at which an eavesdropper steals the private information are denoted as

$$\gamma_{e,1} = \frac{\left|\mathbf{h}_{r,e}^H \boldsymbol{\Theta}\mathbf{H}_{sR} \cdot \boldsymbol{\omega}_1\right|^2}{\left|\mathbf{h}_{r,e}^H \boldsymbol{\Theta}\mathbf{H}_{sR} \cdot \boldsymbol{\omega}_2\right|^2 + \left|\mathbf{h}_{r,e}^H \boldsymbol{\Theta}\mathbf{H}_{sR} \cdot \boldsymbol{\omega}_0\right|^2 + \sigma^2}, \quad (13a)$$

$$\gamma_{e,2} = \frac{\left|\mathbf{h}_{r,e}^H \boldsymbol{\Theta}\mathbf{H}_{sR} \cdot \boldsymbol{\omega}_2\right|^2}{\left|\mathbf{h}_{r,e}^H \boldsymbol{\Theta}\mathbf{H}_{sR} \cdot \boldsymbol{\omega}_1\right|^2 + \left|\mathbf{h}_{r,e}^H \boldsymbol{\Theta}\mathbf{H}_{sR} \cdot \boldsymbol{\omega}_0\right|^2 + \sigma^2}, \quad (13b)$$

$$R_{e,1} = B\log_2\left(1+\gamma_{e,1}\right), R_{e,2} = B\log_2\left(1+\gamma_{e,2}\right). \quad (13c)$$

Thus the information security rate for both users can be presented as

$$R_{s,1} = [R_{p,1} - R_{e,1}]^+, \quad (14a)$$

$$R_{s,2} = [R_{p,2} - R_{e,2}]^+, \quad (14b)$$

where $[\mathrm{X}]^+ = \max\{\mathrm{X}, 0\}$.

### *B. Problem Formulation*

For enhancing the security performance of the downlink RSMA network, this paper presents a total optimization problem that aims at sum information security rate (SISR) maximization. The beamforming matrix is defined as $\mathbf{W} = \left[\boldsymbol{\omega}_0, \boldsymbol{\omega}_1, \boldsymbol{\omega}_2\right]$, and the problem is formulated as

$$\mathbf{P1}: \max_{\mathbf{W},\boldsymbol{\Theta},\mathbf{L}} \sum_{k=1}^{2} R_{s,k} \quad (15a)$$

$$\text{s.t.} \quad \mathrm{C1}: R_{s,k} \ge 0, k \in \{1,2\}, \quad (15b)$$

$$\mathrm{C2}: \|\boldsymbol{\omega}_0\|^2 + \sum_{k=1}^{2}\|\boldsymbol{\omega}_k\|^2 \le P_{BS}, \quad (15c)$$

$$\mathrm{C3}: \varphi_i \in [0, 2\pi), i \in \{1,2,\ldots,M\}, \quad (15d)$$

$$\mathrm{C4}: \mathbf{L} \in \mathcal{X} \otimes \mathcal{Y}, \quad (15e)$$

where $P_{BS}$ is the maximum transmit power.

In $\mathbf{P1}$, constraint (15b) stipulates the minimum threshold of information security rate for ground users, thereby ensuring information security. Constraint (15c) is the source base station transmit power limit. The constraint (15d) represents the phase shift range for RIS reflective element. Constraint (15e) indicates that the UAV cannot exceed the specified area. It is worth noting that the three variables in problem $\mathbf{P1}$ are strongly interrelated and the objective function (15a) is a non-convex, posing significant challenges for solution. Therefore, we decouple the optimization problem into three sub-problems and solve it by iteratively optimizing the beamforming matrix $\mathbf{W}$, RIS phase shift matrix $\boldsymbol{\Theta}$, and UAV position $\mathbf{L}$ respectively.

The notations utilized in this paper are summarized in Table I.

## III. Sum Secrecy Rate Maximization

In this section, we initially apply the SCA algorithm to optimize the beamforming vectors, followed by employing the SDR algorithm to obtain the optimal RIS phase shift matrix. A iteration framework is proposed to jointly optimize above two variables. Subsequently, based on the obtained optimal $\mathbf{W}$ and $\boldsymbol{\Theta}$, we utilize the DDPG algorithm to derive the optimal position of the UAV. Finally, the AO framework is designed for realizing sum information security rate maximization.

TABLE I
NOTATIONS USED IN THIS PAPER.

| Parameter | Definition |
|---|---|
| $\boldsymbol{\omega}_0$, $\boldsymbol{\omega}_1$, $\boldsymbol{\omega}_2$ | Beamforming vectors of public information and private information |
| $\mathbf{h}_k^{LoS}$, $\mathbf{h}_k^{LoS}$ | Los and NLoS components of channel |
| $\mathbf{a}_s$, $\mathbf{a}_R$ | Antenna responses of SBS and RIS |
| $\mathbf{h}_{r,k}$ | Channel from RIS to ground user $k$ |
| $\boldsymbol{\Theta}$ | The phase shift matrix of RIS |
| $\mathbf{H}_{\mathrm{SR}}$ | Channel from SBS to RIS |
| $\gamma_{p,k}$ | SINR of user $k$ receiving private information |
| $\gamma_{e,k}$ | SINR of eavesdropping user $k$ |
| $R_{p,k}$ | Information rate of user $k$ |
| $R_{e,k}$ | Eavesdropping rate of user $k$ |
| $P_{BS}$ | Maximum transmit power of SBS |
| $\mathbf{h}_{r,k}^{\mathrm{H}}$ | Conjugate transpose of the channel $\mathbf{h}_{r,k}$ |
| $\Re\{x\}$ | The real part of the complex number $x$ |

### A. Beamforming Optimization Based on SCA

Given that RIS phase shift matrix $\boldsymbol{\Theta}$ and UAV position $\mathbf{L}$, the optimization problem related to $\mathbf{W}$ is formulated as

$$\mathbf{P2}: \max_{\mathbf{W}} \sum_{k=1}^{2} R_{s,k} \tag{16a}$$

$$\text{s.t. } R_{p,k} \geq R_{e,k}, k \in \{1,2\}, \tag{16b}$$

$$\|\boldsymbol{\omega}_0\|^2 + \sum_{k=1}^{2} \|\boldsymbol{\omega}_k\|^2 \leq P_{BS}, \tag{16c}$$

To facilitate the solution, we introduce the auxiliary variable $\boldsymbol{\delta} = \left[\delta_1, \delta_2, \delta_{e,1}, \delta_{e,1}\right]$, which denotes the achievable information rate for the users and the eavesdropper decoding the private information, then the problem $\mathbf{P2}$ is reformulated as

$$\mathbf{P2.1}: \max_{\mathbf{W},\boldsymbol{\delta}} \sum_{k=1}^{2} (\delta_k - \delta_{e,k}) \tag{17a}$$

$$\text{s.t. } \delta_k \geq \delta_{e,k}, \tag{17b}$$

$$1 + \gamma_{p,k} \geq 2^{\delta_k}, \tag{17c}$$

$$1 + \gamma_{e,k} \leq 2^{\delta_{e,k}}, \tag{17d}$$

$$\|\boldsymbol{\omega}_0\|^2 + \sum_{k=1}^{2} \|\boldsymbol{\omega}_k\|^2 \leq P_{BS}, \tag{17e}$$

There is $k \in \{1,2\}$ in the above formula, and the following is also applicable and will not be explained again. It is not difficult to see that constraints (17c) and (17d) are still non-convex. For dealing with the non-convexity of constraints, the auxiliary variable $\boldsymbol{\lambda} = [\lambda_1, \lambda_2, \lambda_{e,1}, \lambda_{e,2}]$ is introduced to represent the SINR of the ground user $k$ and the eavesdropper eavesdropping on the user's private information. Then the optimization problem $\mathbf{P2.1}$ is reconstructed as

$$\mathbf{P2.2}: \max_{\mathbf{W},\boldsymbol{\delta},\boldsymbol{\lambda}} \sum_{k=1}^{2} (\delta_k - \delta_{e,k}) \tag{18a}$$

$$\text{s.t. } 1 + \lambda_k \geq 2^{\delta_k}, \tag{18b}$$

$$1 + \lambda_{e,k} \leq 2^{\delta_{e,k}}, \tag{18c}$$

$$\frac{\left|\mathbf{h}_{r,k}^H \boldsymbol{\Theta} \mathbf{H}_{\mathrm{SR}} \cdot \boldsymbol{\omega}_k\right|^2}{\left|\mathbf{h}_{r,k}^H \boldsymbol{\Theta} \mathbf{H}_{\mathrm{SR}} \cdot \boldsymbol{\omega}_i\right|^2 + \sigma^2} \geq \lambda_k, i \neq k, \tag{18d}$$

$$\frac{\left|\mathbf{h}_{r,e}^H \boldsymbol{\Theta} \mathbf{H}_{\mathrm{SR}} \cdot \boldsymbol{\omega}_k\right|^2}{\left|\mathbf{h}_{r,e}^H \boldsymbol{\Theta} \mathbf{H}_{\mathrm{SR}} \cdot \boldsymbol{\omega}_i\right|^2 + \left|\mathbf{h}_{r,e}^H \boldsymbol{\Theta} \mathbf{H}_{\mathrm{SR}} \cdot \boldsymbol{\omega}_0\right|^2 + \sigma^2} \leq \lambda_{e,k}, \tag{18e}$$

$$(17b), (17e),$$

However, since the constraints (18c)-(18e) are still non-convex and difficult to handle. Then, a first-order Taylor expansion is used to linearly approximate the constraint (18c) as

$$\mathrm{C5}: 1 + \lambda_{e,k} \leq 2^{\delta_{e,k}^{(r)}} \left[1 + \ln 2 \left(\delta_{e,k} - \delta_{e,k}^{(r)}\right)\right], \tag{19}$$

where $\delta_{e,k}^{(r)}$ denotes the value of $\delta_{e,k}$ obtained in the $r$-th iteration. Next, we introduce the auxiliary variable $\boldsymbol{\beta} = [\beta_1, \beta_2]$ to deal with constraint (18d), which represents the interference noise suffered by the user when decoding private information. The denominator of constraint (18d) is replaced with this variable and then the convex differential form of (18d) can be expressed as

$$\frac{\left|\mathbf{h}_{r,k}^H \boldsymbol{\Theta} \mathbf{H}_{\mathrm{SR}} \cdot \boldsymbol{\omega}_k\right|^2}{\beta_k} \geq \lambda_k, \tag{20}$$

$$\mathrm{C6}: \left|\mathbf{h}_{r,k}^H \boldsymbol{\Theta} \mathbf{H}_{\mathrm{SR}} \cdot \boldsymbol{\omega}_i\right|^2 + \sigma^2 \leq \boldsymbol{\beta}_k, i \neq k, \tag{21}$$

We perform a first-order Taylor expansion of the left-hand side of (20) at point $\left(\boldsymbol{\omega}_k^{(r)}, \beta_k^{(r)}\right)$ to obtain its lower bound, which makes the constraint (20) approximately a convex constraint, so the constraint (20) can be rewritten as

$$\begin{cases} \frac{\left|\mathbf{h}_{r,k}^H \boldsymbol{\Theta} \mathbf{H}_{\mathrm{SR}} \cdot \omega_k\right|^2}{\beta_k} \geq \Gamma\left(\boldsymbol{\omega}_\kappa\right), \\ \Gamma\left(\boldsymbol{\omega}_\kappa\right) \triangleq \frac{2\Re\left\{\left(\boldsymbol{\omega}_k^{(r)}\right)^{\mathrm{H}} \mathbf{h}_k^{\mathrm{H}} \mathbf{h}_k \boldsymbol{\omega}_k\right\}}{\beta_\kappa^{(r)}} - \frac{\left|\mathbf{h}_k \boldsymbol{\omega}_k^{(r)}\right|^2 \beta_k}{\left[\beta_\kappa^{(r)}\right]^2}. \end{cases} \tag{22}$$

Therefore, we only need to ensure that the lower bound $\Gamma\left(\boldsymbol{\omega}_\kappa\right)$ of $\frac{\left|\mathbf{h}_{r,k}^H \boldsymbol{\Theta} \mathbf{H}_{\mathrm{SR}} \cdot \omega_k\right|^2}{\beta_k}$ is not less than $\lambda_k$, that is, the constraint (20) can ultimately be expressed as

$$\mathrm{C7}: \frac{2\Re\left\{\left(\boldsymbol{\omega}_k^{(r)}\right)^{\mathrm{H}} \mathbf{h}_k^{\mathrm{H}} \mathbf{h}_k \boldsymbol{\omega}_k\right\}}{\beta_\kappa^{(r)}} - \frac{\left|\mathbf{h}_k \boldsymbol{\omega}_k^{(r)}\right|^2 \beta_k}{\left[\beta_\kappa^{(r)}\right]^2} \geq \lambda_k. \tag{23}$$

Similarly, through the first-order Taylor expansion constraint (18e) can be reconstructed as

$$\mathrm{C8}: \lambda_{e,k}^{(r)} \sum_{i=0, i\neq k}^{2} \left(2\Re\left\{\left(\boldsymbol{\omega}_i^{(r)}\right)^{\mathrm{H}} \mathbf{h}_e^{\mathrm{H}} \mathbf{h}_e \boldsymbol{\omega}_i\right\} - \left|\mathbf{h}_e \boldsymbol{\omega}_i^{(r)}\right|^2\right) + \lambda_{e,k} \left(\sum_{i=0, i\neq k}^{2} \left|\mathbf{h}_e^H \boldsymbol{\omega}_i^{(r)}\right|^2 + \sigma^2\right) \geq \left|\mathbf{h}_e \boldsymbol{\omega}_k\right|^2. \tag{24}$$

According to the above transformation, the constraints all become convex constraints, so the optimization problem $\mathbf{P2}$

can finally be rewritten as

$$\mathbf{P2.3}: \max_{\mathbf{W},\boldsymbol{\delta},\boldsymbol{\lambda},\boldsymbol{\beta}} \ (\delta_1 - \delta_{e,1} + \delta_2 - \delta_{e,2}) \tag{25a}$$

$$\text{s.t.} \quad \delta_1 \geq \delta_{e,1}, \tag{25b}$$

$$\delta_2 \geq \delta_{e,2}, \tag{25c}$$

$$1 + \lambda_1 \geq 2^{\delta_1}, \tag{25d}$$

$$1 + \lambda_2 \geq 2^{\delta_2}, \tag{25e}$$

$$\text{C2, C5, C6, C7, C8}$$

The original beamforming non-convex optimization problem has been converted to the convex optimization, and then the problem can use convex optimization tools to solve, such as CVX. Please note that there is $k \in \{1, 2\}$ in constraints (C5, C6, C7, C8), that is, since there are two ground users in the communication network, constraints (C5, C6, C7, C8) correspond to 8 constraints during the actual simulation..

### *B. RIS Phase Shift Matrix Optimization Based on SDR*

The beamforming vectors $\boldsymbol{\omega}_0, \boldsymbol{\omega}_1, \boldsymbol{\omega}_2$ are obtained according to the above SCA algorithm, and then fixing beamforming vectors and UAV position $\mathbf{L}$, the RIS phase shift optimization problem can be expressed as

$$\mathbf{P3}: \max_{\boldsymbol{\Theta}} \sum_{k=1}^{2} R_{s,k} \tag{26a}$$

$$\text{s.t. } \varphi_i \in [0, 2\pi), i \in \{1, 2, \ldots, M\}. \tag{26b}$$

Since problem $\mathbf{P3}$ is non-convex and cannot be solved directly using convex optimization tools, the SDR method is employed to solve this problem. Introducing auxiliary variable $\boldsymbol{v} = \left[v_1, v_2, \ldots, v_M\right]^H \in \mathbb{C}^{M\times 1}$, and $v_m = e^{j\varphi_m}, \forall m \in M$, then constraint (26b) can be converted into $|v_m| = 1, m \in M$.

Then, we define

$$\begin{cases} \mathbf{h}_k = \mathbf{h}_{r,k}^{\mathrm{H}} \boldsymbol{\Theta} \mathbf{H}_{\mathrm{SR}} = \boldsymbol{v}^H \mathbf{g}_k, k \in \{1, 2\}, \\ \mathbf{h}_{r,e}^{\mathrm{H}} \boldsymbol{\Theta} \mathbf{H}_{\mathrm{SR}} = \boldsymbol{v}^H \mathbf{g}_e, \end{cases} \tag{27}$$

where

$$\begin{cases} \mathbf{g}_\kappa = diag\big(\mathbf{h}_{r,\kappa}^{\mathrm{H}}\big) \mathbf{H}_{\mathrm{SR}} \in \mathbb{C}^{M\times K}, \\ \mathbf{g}_e = diag\left(\mathbf{h}_{r,e}^{\mathrm{H}}\right) \mathbf{H}_{\mathrm{SR}} \in \mathbb{C}^{M\times K}, \end{cases} \tag{28}$$

and the optimization problem $\mathbf{P3}$ can be represented as

$$\mathbf{P3.1}: \max_{\boldsymbol{v}} \ \sum_{k=1}^{2} B\Big[\log_2\left(1 + C_k\right) - \log_2\left(1 + C_{e,k}\right)\Big] \tag{29a}$$

$$\text{s.t. } \varphi_i \in [0, 2\pi), i \in \{1, 2, \ldots, M\}, \tag{29b}$$

where $k \in \{1, 2\}$, and

$$C_k = \frac{\left|\boldsymbol{v}^H \boldsymbol{g}_k \cdot \boldsymbol{\omega}_k\right|^2}{\sum\limits_{i=1, i\neq k}^{2} \left|\boldsymbol{v}^H \boldsymbol{g}_k \cdot \boldsymbol{\omega}_i\right|^2 + \sigma^2}, \tag{30a}$$

$$C_{e,k} = \frac{\left|\boldsymbol{v}^H \boldsymbol{g}_e \cdot \boldsymbol{\omega}_k\right|^2}{\sum\limits_{i=0, i\neq k}^{2} \left|\boldsymbol{v}^H \boldsymbol{g}_e \cdot \boldsymbol{\omega}_i\right|^2 + \sigma^2}. \tag{30b}$$

The reconstructed problem $\mathbf{P3.1}$ is a quadratic constrained quadratic programming (QCQP) problem and it is difficult to handle due to its non-convexity. SDR technology is used to deal with this problem according to reference [29]. For ground users, let

$$\widetilde{\boldsymbol{v}} = \begin{bmatrix} \boldsymbol{v} \\ 1 \end{bmatrix} \in \mathbb{C}^{(M+1)\times 1}, \boldsymbol{G}_{k,i} = \begin{bmatrix} \boldsymbol{g}_k \boldsymbol{\omega}_i \boldsymbol{\omega}_i^H \boldsymbol{g}_k^H & \mathbf{0}_{M\times 1} \\ \mathbf{0}_{1\times M} & 0 \end{bmatrix}, \tag{31}$$

where

$$\boldsymbol{G}_{1,1} = \begin{bmatrix} \boldsymbol{g}_1 \boldsymbol{\omega}_1 \boldsymbol{\omega}_1^H \boldsymbol{g}_1^H & \mathbf{0}_{M\times 1} \\ \mathbf{0}_{1\times M} & 0 \end{bmatrix}, \tag{32a}$$

$$\boldsymbol{G}_{1,2} = \begin{bmatrix} \boldsymbol{g}_1 \boldsymbol{\omega}_2 \boldsymbol{\omega}_2^H \boldsymbol{g}_1^H & \mathbf{0}_{M\times 1} \\ \mathbf{0}_{1\times M} & 0 \end{bmatrix}, \tag{32b}$$

$$\boldsymbol{G}_{2,1} = \begin{bmatrix} \boldsymbol{g}_2 \boldsymbol{\omega}_1 \boldsymbol{\omega}_1^H \boldsymbol{g}_2^H & \mathbf{0}_{M\times 1} \\ \mathbf{0}_{1\times M} & 0 \end{bmatrix}, \tag{32c}$$

$$\boldsymbol{G}_{2,2} = \begin{bmatrix} \boldsymbol{g}_2 \boldsymbol{\omega}_2 \boldsymbol{\omega}_2^H \boldsymbol{g}_2^H & \mathbf{0}_{M\times 1} \\ \mathbf{0}_{1\times M} & 0 \end{bmatrix}, \tag{32d}$$

There is $\left|\boldsymbol{v}^H \boldsymbol{g}_k \boldsymbol{\omega}_i\right|^2 = \boldsymbol{v}^H \boldsymbol{g}_k \boldsymbol{\omega}_i \boldsymbol{\omega}_i^H \boldsymbol{g}_k^H \boldsymbol{v} = \widetilde{\boldsymbol{v}}^H \boldsymbol{G}_{k,i} \widetilde{\boldsymbol{v}}$, and $\boldsymbol{G} \in \mathbb{C}^{(M+1)\times(M+1)}$.

Similarly for the eavesdropper, there is $\left|\boldsymbol{v}^H \boldsymbol{g}_e \boldsymbol{\omega}_i\right|^2 = \boldsymbol{v}^H \boldsymbol{g}_e \boldsymbol{\omega}_i \boldsymbol{\omega}_i^H \boldsymbol{g}_e^H \boldsymbol{v} = \widetilde{\boldsymbol{v}}^H \boldsymbol{G}_{e,i} \widetilde{\boldsymbol{v}}$, where

$$\boldsymbol{G}_{e,i} = \begin{bmatrix} \boldsymbol{g}_e \boldsymbol{\omega}_i \boldsymbol{\omega}_i^H \boldsymbol{g}_e^H & 0 \\ 0 & 0 \end{bmatrix}, i \in \{0, 1, 2\}. \tag{33}$$

Then, the objective function (29a) is rewritten as

$$\max_{\widetilde{\boldsymbol{v}}} \ B \cdot (D_1 - D_{e,1} + D_2 - D_{e,2}) \tag{34}$$

where

$$D_1 = \log_2\left(1 + \frac{\widetilde{\boldsymbol{v}}^H \boldsymbol{G}_{1,1} \widetilde{\boldsymbol{v}}}{\widetilde{\boldsymbol{v}}^H \boldsymbol{G}_{1,2} \widetilde{\boldsymbol{v}} + \sigma^2}\right), \tag{35a}$$

$$D_2 = \log_2\left(1 + \frac{\widetilde{\boldsymbol{v}}^H \boldsymbol{G}_{2,2} \widetilde{\boldsymbol{v}}}{\widetilde{\boldsymbol{v}}^H \boldsymbol{G}_{2,1} \widetilde{\boldsymbol{v}} + \sigma^2}\right), \tag{35b}$$

$$D_{e,1} = \log_2\left(1 + \frac{\widetilde{\boldsymbol{v}}^H \boldsymbol{G}_{e,1} \widetilde{\boldsymbol{v}}}{\widetilde{\boldsymbol{v}}^H \boldsymbol{G}_{e,2} \widetilde{\boldsymbol{v}} + \widetilde{\boldsymbol{v}}^H \boldsymbol{G}_{e,0} \widetilde{\boldsymbol{v}} + \sigma^2}\right), \tag{35c}$$

$$D_{e,2} = \log_2\left(1 + \frac{\widetilde{\boldsymbol{v}}^H \boldsymbol{G}_{e,2} \widetilde{\boldsymbol{v}}}{\widetilde{\boldsymbol{v}}^H \boldsymbol{G}_{e,1} \widetilde{\boldsymbol{v}} + \widetilde{\boldsymbol{v}}^H \boldsymbol{G}_{e,0} \widetilde{\boldsymbol{v}} + \sigma^2}\right). \tag{35d}$$

Since the problem (34) is still NP-hard, we define $\mathbf{V} = \widetilde{\boldsymbol{v}} \widetilde{\boldsymbol{v}}^H$, where $\mathbf{V}$ is a positive semi-definite matrix. According to reference [34]: $\boldsymbol{x}^T \boldsymbol{U} \boldsymbol{x} = \mathrm{Tr}(\boldsymbol{x}^T \boldsymbol{U} \boldsymbol{x}) = \mathrm{Tr}(\boldsymbol{U} \boldsymbol{x} \boldsymbol{x}^T)$, then the RIS phase shift optimization problem is re-expressed as

$$\mathbf{P3.2}: \max_{\boldsymbol{v}} \ \sum_{k=1}^{2} B\Big[\log_2\left(1 + E_k\right) - \log_2\left(1 + E_{e,k}\right)\Big] \tag{36a}$$

$$\text{s.t. } \mathbf{V}_{m,m} = 1, \forall m = 1, 2, \ldots, M+1, \tag{36b}$$

$$\mathbf{V} \geq 0, \tag{36c}$$

$$rank\left(\mathbf{V}\right) = 1, \tag{36d}$$

where $k \in \{1, 2\}$, and

$$E_k = \frac{\mathrm{Tr}\big(\boldsymbol{G}_{k,k} \mathbf{V}\big)}{\sum\limits_{i=1, i\neq k}^{2} \mathrm{Tr}\big(\boldsymbol{G}_{k,i} \mathbf{V}\big) + \sigma^2}, \tag{37a}$$

$$E_{e,k}=\frac{\mathrm{Tr}\left(\boldsymbol{G}_{e,k}\mathbf{V}\right)}{\sum\limits_{i=0,i\neq k}^{2}\mathrm{Tr}\left(\boldsymbol{G}_{e,i}\mathbf{V}\right)+\sigma^{2}}. \tag{37b}$$

As constraint $rank\left(\mathbf{V}\right)=1$ maintains the non-convex nature of optimization problem $\mathbf{P3.2}$, we combine SDR and SCA techniques to convert the mathematical form of the information security rate of user 1 and user 2 into (37) and (38), where $\mathbf{V}^{(r)}$ denotes the $(M+1)$-dimensional RIS phase shift matrix, that is, the value of $\mathbf{V}$ obtained in the $r$-th iteration.

Therefore, after ignoring the constraint $rank\left(\mathbf{V}\right)=1$, the optimization problem $\mathbf{P3.2}$ can be reformulated as

$$\mathbf{P3.3}:\max_{\mathbf{V}}\ \left(R_{s1}^{'}+R_{s2}^{'}\right) \tag{40a}$$

$$\text{s.t. } \mathbf{V}_{m,m}=1,\forall m=1,2,\ldots,M+1, \tag{40b}$$

$$\mathbf{V}\geq 0. \tag{40c}$$

At this point, problem $\mathbf{P3.3}$ is identified as the convex optimization problem and can be addressed using tools designed for convex optimization, like CVX.

*Gaussian Randomization:* Since we ignore the rank-one constraint for RIS phase shifts optimization, the optimized RIS phase shift matrix $\mathbf{V}\_opt$ don't satisfy the constraint $rank\left(\mathbf{V}\right)=1$. Therefore, how to recover $\boldsymbol{v}$ required by the original optimization problem from the matrix $\mathbf{V}\_opt$ that does not satisfy rank-one is a problem we still need to solve.

A commonly used method is *Gaussian Randomization* [29]. First, the optimized matrix $\mathbf{V}\_opt$ is subjected to eigenvalue decomposition (EVD), i.e., $\mathbf{V}\_opt=\mathbf{Q}\mathbf{\Pi}\mathbf{Q}^{H}$. $\mathbf{Q}$ is the unitary matrix composed of the eigenvectors of the matrix $\mathbf{V}\_opt$, and $\mathbf{\Pi}$ is the diagonal matrix consisting of the eigenvalues, that is, $\mathbf{\Pi}=diag(\Lambda_{1},\Lambda_{2},...,\Lambda_{M+1})$. Second, let $\widetilde{\boldsymbol{v}}=\mathbf{Q}\mathbf{\Pi}^{1/2}\mathbf{r}$, where $\mathbf{r}$ is an $(M+1)$-dimensional column vector, and $\mathbf{r}\in\mathcal{CN}(0,\mathbf{I}_{M+1})$. Then, identify $\widetilde{\boldsymbol{v}}$ corresponding to the maximum objective function among multiple randomly generated $\mathbf{r}$, where $\boldsymbol{v}$ represents the eigenvector associated with the maximum eigenvalue of the matrix $\mathbf{V}\_opt$. Finally, there is $\boldsymbol{v}=e^{j\arg(\vartheta)}$, where $\vartheta=\left[\frac{\tilde{v}}{\tilde{v}_{M+1}}\right]_{(1:M)}$, and $[\mathbf{\Psi}]_{(\mathbf{1:M})}$ represents the new vector composed of the first $M$ elements of vector $\mathbf{\Psi}$. Algorithm 1 gives the details of RIS phase shift optimization based on SDR.

**Algorithm 1** RIS phase shift optimization based on SDR.

1: Given the transmit beamforming vectors $\boldsymbol{\omega}_{0},\boldsymbol{\omega}_{1},\boldsymbol{\omega}_{2}$ and UAV position $\mathbf{L}$, $H_u$.
2: **Initialize** the initial RIS phase shift matrix $\mathbf{\Theta}^{(0)}$, $\mathbf{V}^{(0)}$.
3: **Repeat:**
4: Optimize RIS phase shift $\mathbf{V}$ using SDR algorithm according to (40).
5: Obtain the matrix $\mathbf{V}\_opt$ based on EVD.
6: Obtain the RIS phase shift matrix that satisfies the rank-one constraint based on Gaussian randomization.
7: **Until:** The objective function (40) converges.
8: Output the optimal RIS phase shift matrix $\mathbf{\Theta}$.

### C. UAV Position Optimization Based on DDPG Algorithm

The beamforming vectors $\boldsymbol{\omega}_{0}$, $\boldsymbol{\omega}_{1}$, $\boldsymbol{\omega}_{2}$ and RIS phase shift matrix $\mathbf{\Theta}$ are obtained according to algorithm 1, and then UAV position optimization problem can be denoted as

$$\mathbf{P3}:\max_{\mathbf{L}}\sum_{k=1}^{2}R_{s,k} \tag{41a}$$

$$\text{s.t. } R_{s,k}\geq 0,k\in\{1,2\}, \tag{41b}$$

$$\mathbf{L}\in\mathcal{X}\otimes\mathcal{Y}. \tag{41c}$$

It is not difficult to see that the SISR is highly coupled with the UAV position, and the air-to-ground channel also changes with the UAV position. Therefore, when the UAV is moving, it not only needs to know its own position but also engage with the environment to update the relative position to obtain the channel status information. Meanwhile, if we want to find the optimal position that maximizes SISR during UAV motion, a large amount of UAV position information needs to be stored and compared with the corresponding information security rate. The optimization is difficult, and traditional optimization algorithms are difficult to handle such a massive data stream.

Currently, reinforcement learning can interact with the environment in real-time, enabling parameter updates and continuous learning. Neural networks are used for action selection and decision-making, and constant iterative optimization is performed to explore optimal action to maximize rewards. For the problem that the large amount of data flow generated during the training process is difficult to handle, deep learning can be used to store training data by establishing the experience replay buffer and optimizing the training accuracy based on reinforcement learning. The traditional deep reinforcement learning (DRL) algorithm-Deep Q network (DQN) discretizes actions to simulate continuous actions. But when it is discretized, it will lose training accuracy has limited capabilities, and cannot solve continuous control problems well. Therefore, we use the currently popular DRL algorithm-DDPG algorithm to optimize the UAV position. DDPG is a DRL algorithm that operates on the foundation of the actor-critic architecture. It amalgamates the strengths of the DQN algorithm and uses dual neural networks on this basis. In DDPG, the actor-network engages with the environment to make decisions, while the critic network is used to evaluate the quality of the action. Therefore, compared with DQN, which is mainly suitable for discrete action spaces, DDPG can effectively handle continuous action decision-making problems. The DDPG algorithm framework is shown in Fig. 3.

The DDPG algorithm consists of four components: environment, action, state, and reward. The four elements in the system model we studied are

- ***Environment:*** The environment of this paper is the channel model and downlink dual-user RSMA model. Based on the location information of the ground base station and users, the channel status information is then obtained based on the UAV's own location.
- ***Action:*** During the movement of the UAV, we define action selection as two action dimensions: angle and displacement. The displacement depends on the UAV

$$R_{s1}^{'}=\frac{B}{\ln 2}\times\left\{\begin{array}{l}\ln\left[\frac{1}{\sigma^2}\mathrm{Tr}\left(\boldsymbol{G}_{1,1}\mathbf{V}+\boldsymbol{G}_{1,2}\mathbf{V}\right)+1\right]+\ln Y_1+1+\ln\left[\frac{1}{\sigma^2}\mathrm{Tr}\left(\boldsymbol{G}_{e,0}\mathbf{V}+\boldsymbol{G}_{e,2}\mathbf{V}\right)+1\right]\\-Y_1\cdot\left[\frac{1}{\sigma^2}\mathrm{Tr}\left(\boldsymbol{G}_{1,2}\mathbf{V}\right)+1\right]-Y_{e,1}\cdot\left[\frac{1}{\sigma^2}\mathrm{Tr}\left(\boldsymbol{G}_{e,0}\mathbf{V}+\boldsymbol{G}_{e,1}\mathbf{V}+\boldsymbol{G}_{e,2}\mathbf{V}\right)+1\right]+\ln Y_{e,1}+1\end{array}\right\},\tag{37}$$

$$R_{s2}^{'}=\frac{B}{\ln 2}\times\left\{\begin{array}{l}\ln\left[\frac{1}{\sigma^2}\mathrm{Tr}\left(\boldsymbol{G}_{2,2}\mathbf{V}+\boldsymbol{G}_{2,1}\mathbf{V}\right)+1\right]+\ln Y_2+1+\ln\left[\frac{1}{\sigma^2}\mathrm{Tr}\left(\boldsymbol{G}_{e,0}\mathbf{V}+\boldsymbol{G}_{e,1}\mathbf{V}\right)+1\right]\\-Y_2\cdot\left[\frac{1}{\sigma^2}\mathrm{Tr}\left(\boldsymbol{G}_{2,1}\mathbf{V}\right)+1\right]-Y_{e,2}\cdot\left[\frac{1}{\sigma^2}\mathrm{Tr}\left(\boldsymbol{G}_{e,0}\mathbf{V}+\boldsymbol{G}_{e,1}\mathbf{V}+\boldsymbol{G}_{e,2}\mathbf{V}\right)+1\right]+\ln Y_{e,2}+1\end{array}\right\},\tag{38}$$

where

$$Y_1=\left[\frac{1}{\sigma^2}\mathrm{Tr}\left(\boldsymbol{G}_{1,2}\mathbf{V}^{(r)}\right)+1\right]^{-1},Y_2=\left[\frac{1}{\sigma^2}\mathrm{Tr}\left(\mathbf{G}_{2,1}\mathbf{V}^{(r)}\right)+1\right]^{-1},\tag{39a}$$

$$Y_{e,1}=Y_{e,2}=\left[\frac{1}{\sigma^2}\mathrm{Tr}\left(\boldsymbol{G}_{e,0}\mathbf{V}^{(r)}+\boldsymbol{G}_{e,1}\mathbf{V}^{(r)}+\boldsymbol{G}_{e,2}\mathbf{V}^{(r)}\right)+1\right]^{-1}.\tag{39b}$$

flight speed $\upsilon$ and the length of each time slot $\frac{T}{N}$. The angle between UAV and the $x$-axis positive is expressed as $\psi$. Thus, based on the position $[x[n],y[n]]$, the position of UAV in the $(n+1)$ time slot can be presented as

$$x\left[n+1\right]=x\left[n\right]+\upsilon\cdot\frac{T}{N}\cdot\cos\psi,\tag{42a}$$

$$y\left[n+1\right]=y\left[n\right]+\upsilon\cdot\frac{T}{N}\cdot\sin\psi,\tag{42b}$$

where the displacement can be obtained from $\upsilon\cdot\frac{T}{N}$.

- ***State:*** The current two-dimensional position information $(x[n],y[n])$ of the UAV is used as the state information, that is, the set of all possible positions of the UAV in all time slots is used as the state information.
- ***Reward:*** According to the state and the action generated by the actor-network, these are utilized as input parameters for the critic network to compute the reward for the corresponding time slot. Subsequently, the rewards corresponding to the UAV position across all time slots are aggregated to derive the reward value for the episode. In this paper, the reward is expressed as

$$r(t)=\left\{\begin{array}{l}\sum\limits_{k=1}^{2}R_{s,k},within\mathcal{X}\otimes\mathcal{Y}\\-\frac{1}{2}\sum\limits_{k=1}^{2}R_{s,k},beyond\mathcal{X}\otimes\mathcal{Y}\end{array}\right.,\tag{43}$$

and the total reward is $\boldsymbol{R}=\sum\limits_{t=1}^{N}r(t)$.

In the DDPG algorithm, the actor online network firstly engages with the environment to obtain state information, then takes the state as input and generates the corresponding action under the influence of random noise. Secondly, the obtained state and action serve as input parameters for critic online network and generate the Q-value according to the Bellman equation

$$Q^{\pi}\left(s_t,a_t\right)=E\left[r_t+\varsigma Q^{\pi}\left(s_{t+1},\pi\left(s_{t+1}\right)\right)\right],\tag{44}$$

where $\varsigma\in(0,1]$ represents the reward discount factor. Then the critic online network strategy $\theta^{Q}$ is updated by reducing

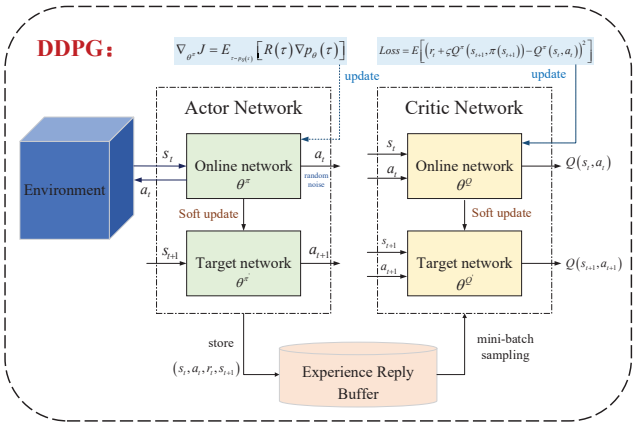


Fig. 3. The DDPG algorithm framework.

the loss function, that is the discrepancy between the evaluation and target values, while the actor online network updates $\theta^{\pi}$ by optimizing the cumulative expectation, that is, the policy gradient. The loss function and policy gradient are expressed as

$$Loss=E\left[\left(r_t+\varsigma Q^{\pi}\left(s_{t+1},\pi\left(s_{t+1}\right)\right)-Q^{\pi}\left(s_t,a_t\right)\right)^2\right],\tag{45a}$$

$$\nabla_{\theta^{\pi}}J=E_{\tau\sim p_{\theta}(\tau)}\left[R\left(\tau\right)\nabla p_{\theta}\left(\tau\right)\right],\tag{45b}$$

where $R\left(\tau\right)=\sum\limits_{t=1}^{N}r_t$, $p_{\theta}\left(\tau\right)$ is the probability distribution function of state $s$ based on action policy $\pi_{\theta}$, and $p_{\theta}\left(\tau\right)=p\left(s_1\right)\prod\limits_{t=1}^{N}p_{\theta}\left(a_t|s_t\right)p\left(s_{t+1}|s_t,a_t\right)$.

The two target networks, do not participate in environmental interaction during the training and learning process and do not update in real-time with the online network. Instead, they perform soft updates at regular intervals while ensuring accuracy and algorithm convergence. The update method is as

follows.

$$\begin{cases} \theta^{Q'} \leftarrow \varepsilon\theta^{Q} + (1-\varepsilon)\,\theta^{Q'}, \\ \theta^{\pi'} \leftarrow \varepsilon\theta^{\pi} + (1-\varepsilon)\,\theta^{\pi'}, \end{cases} \tag{46}$$

where the value range of the soft update factor is $\varepsilon \in (0, 1]$.The DDPG optimization is summarized in Algorithm 2.

**Algorithm 2** UAV Position Optimization Based on DDPG.

**Set** the environment, UAV initial position, episode $E$ and experience replay buffer capacity $M_U$.
**Initialization** online network parameters $\pi$, $Q$ and target network parameters $\pi'$, $Q'$, update factors $\varsigma$, $\varepsilon$,
**for** $r = 1 : E$ **do**
  Actor online network interacts with the environment to obtain the current UAV state.
  Choose action based on $a_t = \pi(s_t, \theta^{\pi}) + N_{random}$.
  Obtain $\mathbf{\Theta}^{(r)}$ using Gaussian randomization.
  Calculate reward and store $(a_t, s_t, r_t, s_{t+1})$ in experience reply buffer.
  Randomly sample small volumes of data and calculate the Q value.
  Update online network parameters according to (45).
  Update target network parameters according to (46).
**end for**
Output the optimal UAV position and reward.

### D. Overall Algorithm Framework

Leveraging the aforementioned solution, we optimize the beamforming vectors using SCA method and the RIS phase shift matrix using SDR technology. Consequently, an iterative algorithm is devised for jointly optimizing the beamforming and RIS phase shift matrix.

The iteration algorithm is detailed in Algorithm 3. Specifically, we first initialize and perform beamforming optimization based on the initial values. Second, following the optimized beamforming vectors, the SDR technique is applied to obtain the RIS phase shift matrix, and Gaussian randomization is performed to restore a solution that meets the constraint $rank\,(\mathbf{V}) = 1$. Finally, it is judged whether the difference between the sum information security rate calculated from the iteration result and the sum information security rate corresponding to the initial value satisfies the convergence threshold. If so, the optimal beamforming vectors and RIS phase shift matrix will be output; otherwise, variable assignment is performed until the convergence threshold is achieved or at the maximum number of iterations, at which point the loop terminates. The optimal beamforming vectors and RIS phase shift matrix are obtained.

Then, the optimal beamforming vector and RIS phase shift, as derived from Algorithm 3, are utilized as environmental parameter inputs, and the DDPG algorithm is used to optimize the UAV position according to section III-C. Finally, we design an overall AO framework for joint optimization, sequentially addressing the three variables - the beamforming vectors, RIS phase shift matrix and UAV position. The overall algorithm framework of the proposed scheme is depicted in Fig. 4.

**Algorithm 3** Iteration Algorithm.

**Initialization**
  Given UAV position $\mathbf{L}$ and $H_u$.
  Initialize $\boldsymbol{\omega}_0^{(0)}$, $\boldsymbol{\omega}_1^{(0)}$, $\boldsymbol{\omega}_2^{(0)}$, $\mathbf{\Theta}^{(0)}$, $\mathbf{V}^{(0)}$.
  Set the number of iterations $I_{\max}$.
  Set convergence threshold $\zeta = 2 \times 10^{-3}$.
**for** $r = 1 : I_{\max}$ **do**
  Obtain $\boldsymbol{\omega}_0^{(r)}$, $\boldsymbol{\omega}_1^{(r)}$, $\boldsymbol{\omega}_2^{(r)}$ from (25) using SCA.
  According to $\boldsymbol{\omega}_0^{(r)}$, $\boldsymbol{\omega}_1^{(r)}$, $\boldsymbol{\omega}_2^{(r)}$, obtain $\mathbf{V}^{(r)}$ from (40) using SDR.
  Obtain $\mathbf{\Theta}^{(r)}$ using Gaussian randomization.
  Calculate $R_s^{(r)}$ corresponding to $\boldsymbol{\omega}_0^{(r)}$, $\boldsymbol{\omega}_1^{(r)}$, $\boldsymbol{\omega}_2^{(r)}$, $\mathbf{\Theta}^{(r)}$.
  **if** $\left|R_s^{(r)} - R_s^{(r-1)}\right| > \zeta$ **then**
    update variables $\boldsymbol{\omega}_0^{(r-1)} \leftarrow \boldsymbol{\omega}_0^{(r)}$, $\boldsymbol{\omega}_1^{(r-1)} \leftarrow \boldsymbol{\omega}_1^{(r)}$, $\boldsymbol{\omega}_2^{(r-1)} \leftarrow \boldsymbol{\omega}_2^{(r)}$.
    update variables $\mathbf{\Theta}^{(r-1)} \leftarrow \mathbf{\Theta}^{(r)}$, $\mathbf{V}^{(r-1)} \leftarrow \mathbf{V}^{(r)}$.
    **repeat** from step 6.
  **else**
    Output the optimal $\boldsymbol{\omega}_0^{(*)}$, $\boldsymbol{\omega}_1^{(*)}$, $\boldsymbol{\omega}_2^{(*)}$, $\mathbf{\Theta}^{(*)}$.
  **end if**
**end for**
Output the optimal $\boldsymbol{\omega}_0^{(*)}$, $\boldsymbol{\omega}_1^{(*)}$, $\boldsymbol{\omega}_2^{(*)}$, $\mathbf{\Theta}^{(*)}$.

*Complexity Analysis:* The beamforming vectors are optimized by the SCA algorithm, and the SCA algorithm complexity is $\mathcal{O}\left(P^{3.5}\right)$, where $P$ is the number of updated variables in each iteration. Then we use SDR to optimize the RIS phase shifts and use Gaussian randomization to obtain a solution that meets all constraints. The SDR algorithm complexity [29] is $\mathcal{O}\left(N_{GR}(Z+1)^{4.5}\right)$, where $Z$ represents the number of variables and $N_{GR}$ is the number of Gaussian randomizations. In summary, the complexity of Algorithm 1 is given as $\mathcal{O}(IA) = \mathcal{O}\left(I_{\max}\left(P^{3.5} + N_{GR}(Z+1)^{4.5}\right)\log_2(1/\zeta)\right)$, where $I_{\max}$ is the iterations number of algorithm 1 and $\zeta$ is the convergence threshold. The complexity of the DDPG algorithm is typically associated with the number of episodes, cycles within each episode, mini-batch samples, and the number of neurons. In this paper, the DDPG algorithm complexity is $\mathcal{O}\left(N_e N N_s N_u\right)$, where $N_e$ represents the number of episodes, $N$ is the total number of time slots, $N_s$ is the number of mini-batch samples and the number of neurons is represented as $N_u = (2 \times N_h + N_h \times 2) + (2 \times N_h + N_h \times 1) \times 2$, where $N_h$ refers to the number of hidden layers in the neural network. Therefore, the overall AO framework optimization complexity is $\mathcal{O}\left(N_{AO}\left(\mathcal{O}(IA) + \mathcal{O}\left(N_e N N_s N_u\right)\right)\right)$, where $N_{AO}$ is total number of iterations.

## IV. Simulation Results

### A. Simulation Parameters

For downlink RSMA communication networks, the security performance of the proposed scheme is assessed in this section. First, the influence of the SBS maximum transmit power, the number of RIS reflective elements, and the number of SBS transmit antennas on the system SISR is analyzed. Then the effectiveness of the security rate optimization scheme

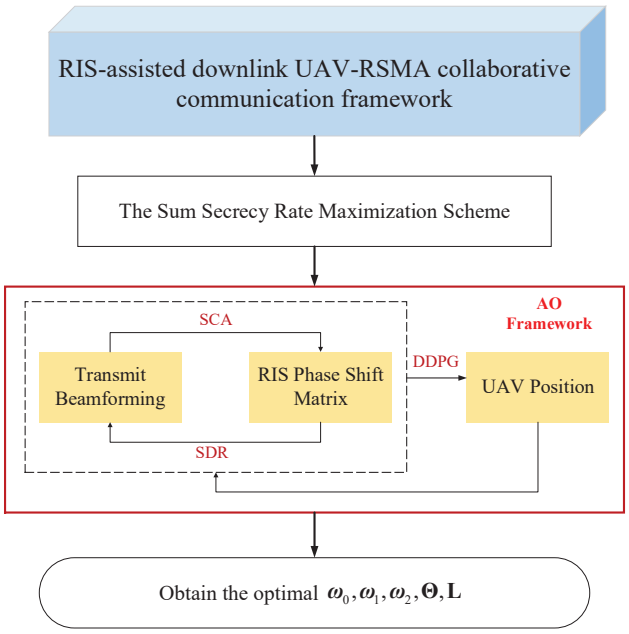


Fig. 4. The overall algorithm framework of the proposed scheme.

based on the DDPG algorithm in this paper is verified. Finally, we compare the proposed scheme with the NOMA scheme and benchmark scheme (random phase shifts) to ascertain its superiority. In the simulation, the coordinates of two users are $[130, 60]$ and $[140, 70]$ respectively. The detailed parameter settings for the simulation are outlined in Table II.

TABLE II
SIMULATION PARAMETERS.

| Parameter | Value |
|---|---|
| Number of transmitting antennas, $K$ | 5 |
| Number of RIS reflective elements, $M$ | 9 |
| Channel gain at $d_0 = 1m$, $\beta_0$ | $5 \times 10^{-4}$ |
| Noise power, $\sigma^2$ | -80 dBm |
| Rice factor, $K_u$ | 6 |
| Maximum transmission power, $P_{BS}$ | 20 dBm |
| Bandwidth, $B$ | 10 Hz |
| UAV height, $H_u$ | 50 m |
| UAV flight speed, $v$ | 10 m/s |
| UAV flight time, $T$ | 200 s |
| UAV initial position | [140, 30] m |
| SBS's location, $\mathbf{L_s}$ | [10, 50] m |
| Env's location, $\mathbf{L_e}$ | [160, 45] m |
| UAV flight area, $\mathcal{X} \otimes \mathcal{Y}$ | $200 \times 200$ m |
| Total time slot, $N$ | 500 |
| Learning rate of actor network | 0.001 |
| Learning rate of critic network | 0.002 |
| Number of hidden layers, $N_h$ | 30 |
| soft update factor | 0.01 |
| Experience replay buffer capacity | 10000 |

## B. Simulation Results

Figure 5 illustrates the relationship between SISR and the number of iterations at different maximum transmit powers. The figure shows that SISR increases with the number of iterations and eventually converges. Moreover, Increasing the maximum transmit power of SBS can enhance the network's security performance. When the maximum transmit power increases, the SBS has more energy to transmit public and private information, thereby improving signal quality and effectively reducing the impact of noise interference. In addition, the SISR corresponding to higher maximum transmit powers converges more slowly. This can be attributed to the larger exploration space and better power allocation of beamforming vectors associated with higher transmit powers. However, when the transmit power is low, such as 15dBm and 16dBm, limited by the local convergence characteristics of the SCA optimization algorithm, the SISR exhibits a rise followed by a decline and finally converges.

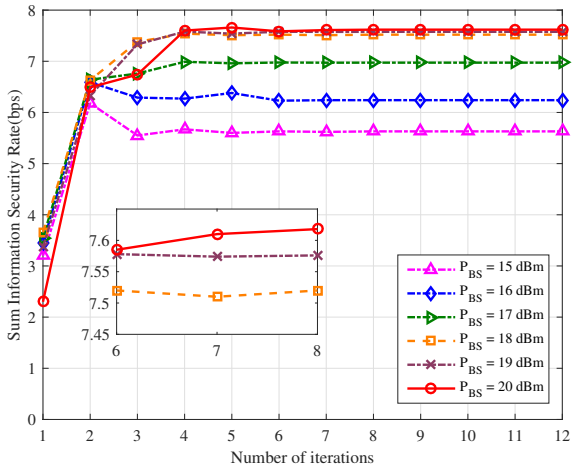


Fig. 5. The SISR versus the number of iterations ($N = 5$, $M = 9$).

Figure 6 presents the effect of varying numbers of RIS reflective elements on SISR. As seen in the figure, it displays an escalating trend in the system's SISR with an increase in the number of RIS reflective elements. Since the intelligent adjustment of phase by RIS can heighten channel gain, more channel subspaces are added between RIS and ground users as the number of RIS elements increases, thereby improving signal quality and information security rate. Notably, the greater the number of RIS reflective elements, the slower the convergence speed, and more reflective elements mean more power consumption and higher optimization complexity. Therefore, it is crucial to select the number of RIS reflective elements judiciously to strike a balance between secure performance and resource utilization. Fig. 7 depicts the correlation between SISR and maximum transmit power for three distinct counts of RIS reflective elements. Specifically, when $M = 16$, the system's SISR can be increased by 85.6% as transmit power rises from 10 dBm to 15 dBm.

Figure 8 illustrates the effect of the SISR versus the number of transmitting antennas. The figure indicates that the system's

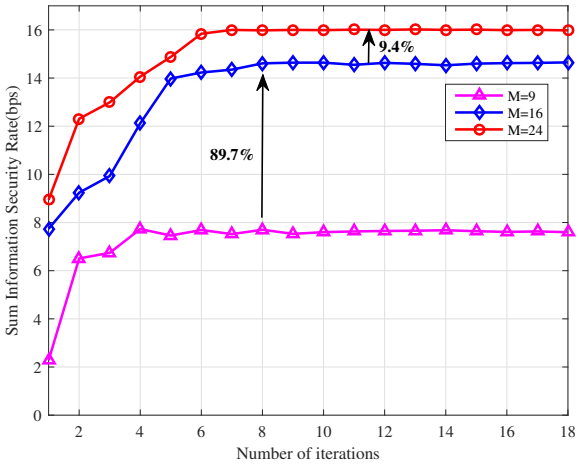


Fig. 6. The SISR versus the number of iterations ($P_{BS} = 20dBm$).

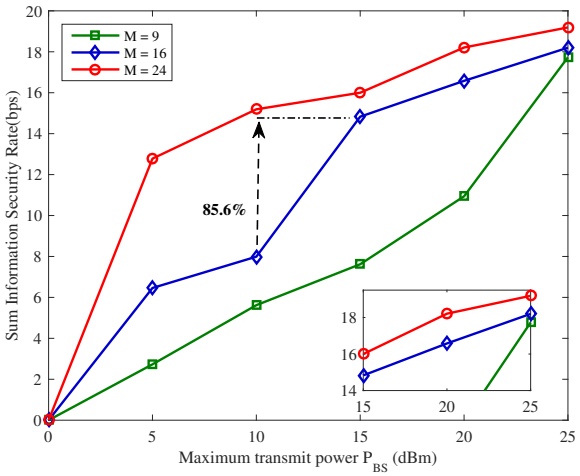


Fig. 7. The SISR versus the maximum transmit power.

SISR escalates with the increase in the count of transmission antennas. This is attributed to the fact that MIMO technology allows multiple transmitting antennas to send information simultaneously, thereby increasing the communication path and ensuring efficient transmission of information. However, it is notable that the larger number of transmitting antennas results in slower convergence speed. This is because the increase in number of transmitting antennas also increases the corresponding count of each beamforming vector element, so it also takes longer when using the alternating iteration framework.

Figure 9 presents the SISR optimization results based on the DDPG algorithm. The UAV trajectory during the actual flight, the relative positions of the SBS, ground user, and the eavesdropper are shown in the figure. The start point of the UAV is $[140, 30]$, and UAV is located between the ground user and the eavesdropper. With the goal of maximizing the system's SISR and ensuring information security, the UAV moves in a direction away from Env, and the optimal position of the UAV is finally found through the proposed

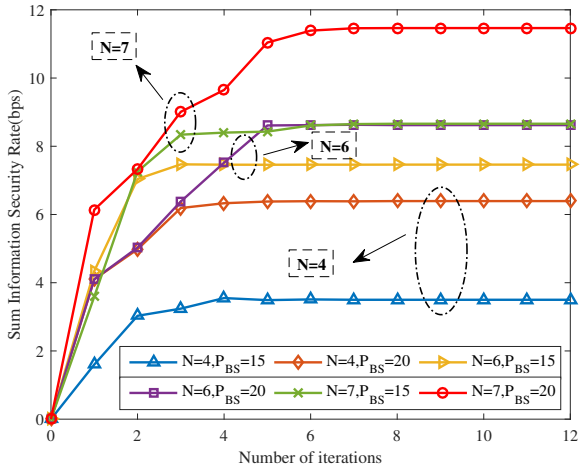


Fig. 8. The SISR versus the number of iterations ($N = 5$, $M = 9$).

DDPG algorithm optimization, which is fixed at the point $[44, 89]$. Its x-coordinate and y-coordinate variations during the optimization process are shown in Fig. 10. The Fig. 10 is the optimization result of the UAV coordinates in the last episode. In the early stage of DDPG optimization, the position of the UAV fluctuated greatly. Through interaction and training with the environment, the UAV has learned the optimal action in the later stage of the episode.

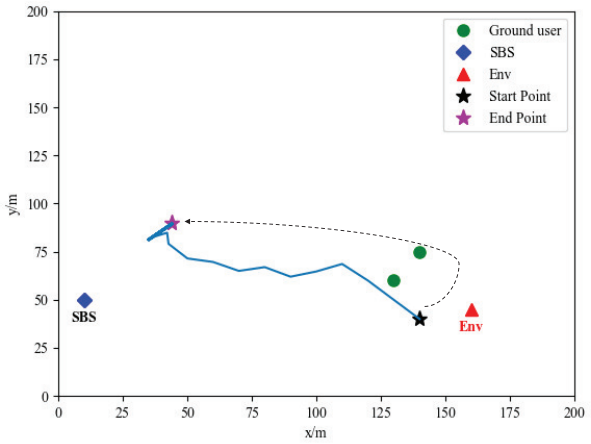


Fig. 9. UAV motion trajectory.

Figure 11 is a reward that is the sum of the corresponding information security rate from the UAV start point to the current position. Since the first few episodes of the DDPG algorithm are training and saving the data in the experience pool, the corresponding rewards fluctuate greatly. In the 20-th episode, because the UAV flew beyond the specified area, the reward value plummeted and dropped to a negative value. Subsequently, with the continuous interaction with the environment, the actor network and critic network within DDPG undergo optimization and updates. The UAV gradually moves in the direction of maximizing the SISR, and finally, the reward

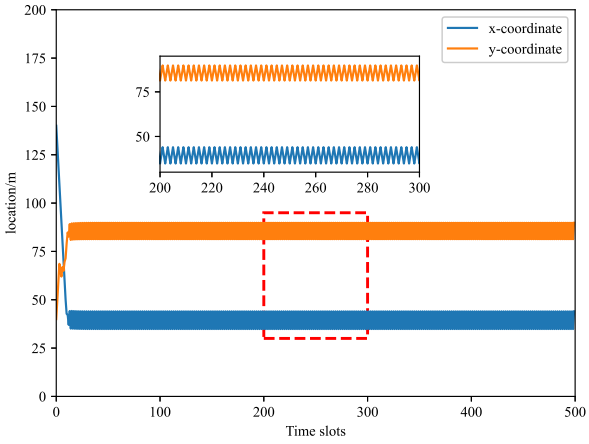


Fig. 10. Coordinate transformation during UAV movement.

reaches convergence.

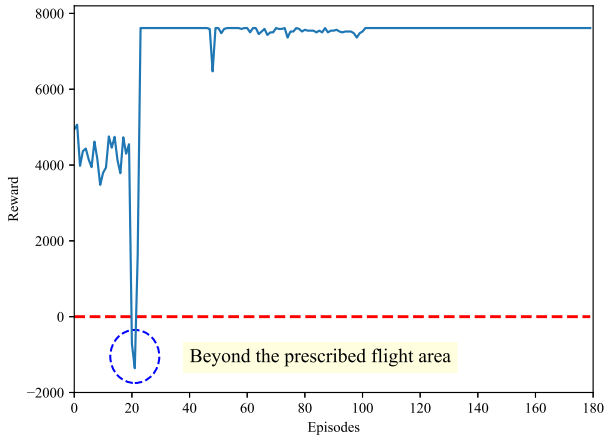


Fig. 11. Convergence of the proposed DDPG algorithm.

Figure 12 is the comparison of security performance (SISR) for three schemes. The SISR of the proposed scheme is observed to have a 29.7% increase compared with the NOMA scheme. Specifically, RSMA first splits the message into public and private information, and the important information is hidden in the private information so that the public information can be used as noise to interfere with the eavesdropper. The NOMA scheme [29] employed SCA and SDR methods for beamforming vectors and RIS phase shifts optimization. Specially, the NOMA scheme completely encodes user 2's message $x_2$ into $x_0$. As a result, user 1 can decode private message only after completely removing the message $x_2$, and user 2 only needs to decode its own message without effectively interfering with the eavesdropper, resulting in the lower security performance. Moreover, the benchmark scheme does not optimize the RIS phase shifts but uses random phase shifts. In the proposed scheme, SDR technology is utilized for optimizing the RIS phase shift matrix, which can enable precise adjustment of the phase of each reflective element to improve reflection accuracy, thus enhancing the signal transmission and improving the SISR of the system.

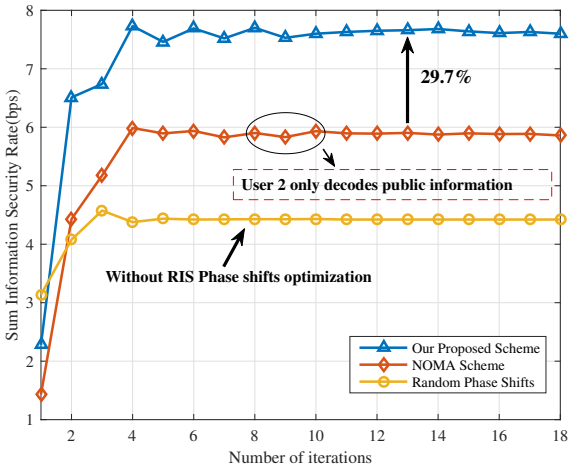


Fig. 12. The comparison of security performance for three schemes($N = 5$, $M = 9$).

## V. Conclusion

In this paper, a novel RIS-assisted UAV-RSMA collaborative communication framework was proposed to enhance the communication security, spectrum efficiency, and multiple access capability of UAV-enabled IoT. Specifically, we first introduced RSMA technology to serve dual users and improve spectrum efficiency. Second, for the issue of information security, a secrecy optimization scheme for maximizing the sum secrecy rate was formulated and solved by jointly optimizing the transmit beamforming, RIS phase shift matrix, and UAV position based on an AO framework. Finally, simulation results validated the superiority of the security scheme in this paper, and we analyzed the impact of various parameters on security performance.

Despite the advancements for the RIS-assisted UAV-RSMA scenario presented in this paper, several issues warrant further investigation. First, the Doppler effect caused by UAV movement can significantly affect the channel characteristics. The Doppler frequency shift may cause signal distortion and increase the bit error rate, so it is necessary to consider the impact of the Doppler effect on the channel, such as the multi-channel environment or rapid fluctuations caused by UAV movement. Second, for highly dynamic environments, potential algorithms that can be used to adapt to the changing channel conditions in dynamic environments should be investigated, such as machine learning techniques, adaptive modulation, coding schemes, or advanced beamforming strategies, to achieve dynamic environment interaction and improve communication performance. Finally, RIS is a promising technology for 6G communication. Currently, STAR-RIS, as a supplement to RIS, can achieve signal reflection and transmission, enabling full-dimensional communication coverage. Therefore, the communication enhancement issue of STAR-RIS applied to multi-user scenarios deserves in-depth research.

## REFERENCES


[1] J. Liu, Y. Shi, Z. M. Fadlullah and N. Kato, "Space-Air-Ground Integrated Network: A Survey," *IEEE Commun. Surv. Tut.*, vol. 20, no. 4, pp. 2714-2741, 2018.

[2] L. Cao and H. Wang, "Research on UAV Network Communication Application Based on 5G Technology," *International Conference on Electronic Communication and Artificial Intelligence (IWECAI)*, Zhuhai, China, 2022, pp. 125-129.

[3] X. Qin, Z. Song, T. Hou, W. Yu, J. Wang and X. Sun, "Joint Optimization of Resource Allocation, Phase Shift, and UAV Trajectory for Energy-Efficient RIS-Assisted UAV-Enabled MEC Systems," *IEEE Transactions on Green Communications and Networking*, vol. 7, no. 4, pp. 1778-1792, Dec. 2023.

[4] S. Chen et al., "Optimal RIS Allocations for PLS With Uncertain Jammer and Eavesdropper," *IEEE Transactions on Consumer Electronics*, vol. 69, no. 4, pp. 927-936, Nov. 2023.

[5] S. Jangsher, A. Al-Dweik, Y. Iraqi, A. Pandey and J. -P. Giacalone, "Group Secret Key Generation Using Physical Layer Security for UAV Swarm Communications," *IEEE Transactions on Aerospace and Electronic Systems*, vol. 59, no. 6, pp. 8550-8564, Dec. 2023.

[6] A. Chauhan, S. Ghosh and A. Jaiswal, "RIS Partition-Assisted Non-Orthogonal Multiple Access (NOMA) and Quadrature-NOMA With Imperfect SIC," *IEEE Transactions on Wireless Communications*, vol. 22, no. 7, pp. 4371-4386, July. 2023.

[7] X. Lyu, S. Aditya, J. Kim and B. Clerckx, "Rate-Splitting Multiple Access: The First Prototype and Experimental Validation of its Superiority over SDMA and NOMA," *IEEE Transactions on Wireless Communications*, to be published, doi: 10.1109/TWC.2024.3367891.

[8] D. Diao, B. Wang, K. Cao, B. Zheng, J. Weng and J. Chen,"Secure RIS Deployment Strategies for Wireless-Powered Multi-UAV Communication," *IEEE Internet of Things Journal*, vol. 11, no. 10, pp. 18154-18166, May. 2024.

[9] S. K. Singh, K. Agrawal, K. Singh, C. -P. Li and Z. Ding, "NOMA Enhanced Hybrid RIS-UAV-Assisted Full-Duplex Communication System With Imperfect SIC and CSI," *IEEE Transactions on Communications*, vol. 70, no. 11, pp. 7609-7627, Nov. 2022.

[10] K. Guo and K. An, "On the Performance of RIS-Assisted Integrated Satellite-UAV-Terrestrial Networks With Hardware Impairments and Interference," *IEEE Wireless Communications Letters*, vol. 11, no. 1, pp. 131-135, Jan. 2022.

[11] Bansal, N. Agrawal, K. Singh, C. -P. Li and S. Mumtaz, "RIS Selection Scheme for UAV-Based Multi-RIS-Aided Multiuser Downlink Network With Imperfect and Outdated CSI," *IEEE Transactions on Communications*, vol. 71, no. 8, pp. 4650-4664, Aug. 2023.

[12] A. V. Savkin, C. Huang and W. Ni, "Joint Multi-UAV Path Planning and LoS Communication for Mobile-Edge Computing in IoT Networks With RISs," *IEEE Internet of Things Journal*, vol. 10, no. 3, pp. 720-2727, Feb. 2023.

[13] Z. Peng, R. Liu, C. Pan, Z. Zhang and J. Wang, "Energy Minimization for Active RIS-Aided UAV-Enabled SWIPT Systems," *IEEE Communications Letters*, to be published, doi:10.1109/LCOMM.2024.3389990.

[14] A. B. M. Adam et al., "Intelligent and Robust UAV-Aided Multiuser RIS Communication Technique With Jittering UAV and Imperfect Hardware Constraints," *IEEE Transactions on Vehicular Technology*, vol. 72, no. 8, pp. 10737-10753, Aug. 2023.

[15] D. Wang, M. Wu, Z. Wei, K. Yu, L. Min and S. Mumtaz, "Uplink Secrecy Performance of RIS-Based RF/FSO Three-Dimension Heterogeneous Networks," *IEEE Transactions on Wireless Communications*, vol. 23, no. 3, pp. 1798-1809, March. 2024.

[16] L. Chai, L. Bai, T. Bai, J. Shi and A. Nallanathan, "Secure RIS-Aided MISO-NOMA System Design in the Presence of Active Eavesdropping," *IEEE Internet of Things Journal*, vol. 10, no. 22, pp. 19479-19494, Nov. 2023.

[17] Y. Shang, Y. Peng, R. Ye and J. Lee, "RIS-Assisted Secure UAV Communication Scheme Against Active Jamming and Passive Eavesdropping," *IEEE Transactions on Intelligent Transportation Systems*, vol. 25, no. 11, pp. 16953-16963, Nov. 2024.

[18] Y. Zhou et al., "Secure Multi-Layer MEC Systems With UAV-Enabled Reconfigurable Intelligent Surface Against Full-Duplex Eavesdropper," *IEEE Transactions on Communications*, vol. 72, no. 3, pp. 1565-1577, March. 2024.

[19] H. T. Huong Giang, P. D. Thanh, H. Ko and S. Pack, "Deep Reinforcement Learning-based Power Allocation for Downlink RSMA System," *2022 13th International Conference on Information and Communication Technology Convergence (ICTC)*, Jeju Island, Korea, Republic of, 2022, pp. 775-777.

[20] G. Zhou, Y. Mao and B. Clerckx, "Rate-Splitting Multiple Access for Multi-Antenna Downlink Communication Systems: Spectral and Energy Efficiency Tradeoff," *IEEE Transactions on Wireless Communications*, vol. 21, no. 7, pp. 4816-4828, Jul. 2022.

[21] Z. Yang, M. Chen, W. Saad and M. Shikh-Bahaei, "Optimization of Rate Allocation and Power Control for Rate Splitting Multiple Access (RSMA)," *IEEE Transactions on Communications*, vol. 69, no. 9, pp. 5988-6002, Sept. 2021.

[22] S. K. Singh, K. Agrawal, K. Singh, B. Clerckx and C. -P. Li, "RSMA for Hybrid RIS-UAV-Aided Full-Duplex Communications With Finite Blocklength Codes Under Imperfect SIC," *IEEE Transactions on Wireless Communications*, vol. 22, no. 9, pp. 5957-5975, Sept. 2023.

[23] Y. Gao, Q. Wu, W. Chen and D. W. K. Ng, "Rate-Splitting Multiple Access for Intelligent Reflecting Surface-Aided Secure Transmission," *IEEE Communications Letters*, vol. 27, no. 2, pp. 482-486, Feb. 2023.

[24] S. Lee, S. Park, J. Park and J. Choi, "Rate-Splitting Multiple Access Precoding for Selective Security," *2023 IEEE 97th Vehicular Technology Conference (VTC2023-Spring)*, Florence, Italy, 2023, pp. 1-5.

[25] Y. Lu, "Secrecy Energy Efficiency in RIS-Assisted Networks," *IEEE Transactions on Vehicular Technology*, vol. 72, no. 9, pp. 12419-12424, Sept. 2023.

[26] Z. Yao, W. Cheng, W. Zhang and H. Zhang, "Resource Allocation for 5G-UAV-Based Emergency Wireless Communications," *IEEE Journal on Selected Areas in Communications*, vol. 39, no. 11, pp. 3395-3410, Nov. 2021.

[27] G. Raja and G. Saravanan, "Eco-Friendly Disaster Evacuation Framework for 6G Connected and Autonomous Vehicular Networks," *IEEE Transactions on Green Communications and Networking*, vol. 6, no. 3, pp. 1368-1376, Sept. 2022.

[28] Y. He, D. Wang, F. Huang, R. Zhang, X. Gu and J. Pan, "A V2I and V2V Collaboration Framework to Support Emergency Communications in ABS-Aided Internet of Vehicles," *IEEE Transactions on Green Communications and Networking*, vol. 7, no. 4, pp. 2038-2051, Dec. 2023.

[29] S. Jiao, F. Fang, X. Zhou and H. Zhang, "Joint Beamforming and Phase Shift Design in Downlink UAV Networks with IRS-Assisted NOMA," ," *Journal of Communications and Information Networks*, vol. 5, no. 2, pp. 138-149, June. 2020.

[30] D. Wang et al., "Active Aerial Reconfigurable Intelligent Surface Assisted Secure Communications: Integrating Sensing and Positioning," ," *IEEE Journal on Selected Areas in Communications*, to be published, doi: 10.1109/JSAC.2024.3414621.

[31] J. W. Choi and S. H. Cho, "3D positioning algorithm based on multiple quasi-monostatic IR-UWB radar sensors," ," *2017 IEEE Radar Conference (RadarConf)*, Seattle, WA, USA, 2017, pp. 1531-1535.

[32] J. Feng, X. Liu, Z. Liu and T. S. Durrani, "Optimal Trajectory and Resource Allocation for RSMA-UAV Assisted IoT Communications," *IEEE Transactions on Vehicular Technology*, to be published, doi: 10.1109/TVT.2024.3354329.

[33] K. Chen, Y. Mao, L. Yin, C. Xu and Y. Huang, "Rate-Splitting Multiple Access for Simultaneous Multi-User Communication and Multi-Target Sensing," *IEEE Transactions on Vehicular Technology*, to be published, doi:10.1109/TVT.2024.3383657.

[34] G. Zhou, L. Zhao, G. Zheng, S. Song, J. Zhang and L. Hanzo, "Multiobjective Optimization of Space–Air–Ground-Integrated Network Slicing Relying on a Pair of Central and Distributed Learning Algorithms," *IEEE Internet of Things Journal*, vol. 11, no. 5, pp. 8327-8344, March. 2024.

[35] A. Gao, Q. Wang, Y. Hu, W. Liang and J. Zhang, "Dynamic Role Switching Scheme With Joint Trajectory and Power Control for Multi-UAV Cooperative Secure Communication," *IEEE Transactions on Wireless Communications*, vol. 23, no. 2, pp. 1260-1275, Feb. 2024.

[36] U. A. Mughal, Y. Alkhrijah, A. Almadhor and C. Yuen, "Deep Learning for Secure UAV-Assisted RIS Communication Networks," *IEEE Internet of Things Journal*, vol. 7, no. 2, pp. 38-44, March. 2024.

[37] Z. Guo, K. Yu, N. Kumar, W. Wei, S. Mumtaz and M. Guizani, "Deep-Distributed-Learning-Based POI Recommendation Under Mobile-Edge Networks," *IEEE Internet of Things Journal*, vol. 10, no. 1, pp. 303-317, 1 Jan.1, 2023.

[38] J. Pan et al., "AI-Driven Blind Signature Classification for IoT Connectivity: A Deep Learning Approach," *IEEE Transactions on Wireless Communications*, vol. 21, no. 8, pp. 6033-6047, Aug. 2022.

[39] D. Wang, L. Yuan, H. Zhao, L. Min, and Y. He, "Secure transmission of IRS-UAV buffer-aided relaying system with delay constraint," *Chin. J. Aeronaut.*, Early Access, doi: 10.1016/j.cja.2024.08.006.

[40] Y. He, D. Wang, F. Huang, R. Zhang and L. Min, "Aerial-ground integrated vehicular networks: A UAV-vehicle collaboration perspective," *IEEE Trans. Intell. Transp. Syst.*, vol. 25, no. 6, pp. 5154–5169, Jun. 2024.

**Dawei Wang** (S'14-M'18) received the B.S. degree from University of Jinan, China, in 2011 and the Ph.D. degree from Xi'an Jiaotong University, China in 2018. From 2016 to 2017, he was a Visiting Student with the School of Engineering, The University of British Columbia. He is currently an Associate Professor with the School of Electronics and Information, Northwestern Polytechnical University, Xi'an, China. He has served as Technical Program Committee (TPC) member for many International conferences, such as IEEE GLOBECOM, IEEE ICC, etc. His research interests include Physical-Layer Security, Integrated Sensing and Communication, NOMA Communications, UAV Communications, and Resource Allocation.

**Jiawei Li** received the B.S. degree in communication engineering from Zhengzhou University, Zhengzhou, China, in 2022. She is working toward a Ph.D. in information and communication engineering with Northwestern Polytechnical University, Xi'an, China. Her research interests include UAV communication networks, mobile IoV, machine learning, and physical layer security.

**Qinyi Lv** received the B.S. and Ph.D. degrees from Zhejiang University, Hangzhou, China, in 2013 and 2018, respectively. He is currently an Associate Professor with Northwestern Polytechnical University. His recent research interests include RF systems, microwave circuits, radar detection, and inverse scattering problems.

**Yixin He** received his B.S., M.Sc., and Ph.D. degrees in communication and information engineering from the School of Electronics and Information, Northwestern Polytechnical University, Xian, China, in 2016, 2019, and 2023, respectively. From 2021 to 2022, he was a visiting Ph.D. student with the Department of Computer Science, University of Victoria, Victoria, BC, Canada. He has been a Guest Editor for Journal of Marine Science and Engineering (JMSE) and has served as the TPC member for IEEE VTC 2022. Moreover, he is serving as a reviewer for several international journals and conferences, including IEEE WCL, Globecom, ICC, etc. His research interests include VANETs, resource allocation, and UAV communications.s.

**Li Li** received his B.S. and M.S. degrees from Xidian University China, in 1998 and 2010 , respectively, the M.S. degree from the University of Surrey UK, in 2016, and the Ph.D. degree from Northwestern Polytechnical University, Xi'an, China, in 2022. Currently, he is a professor in Northwestern Polytechnical University. His research interests include data transmission subsystem, advanced satellite communication technology, and spaceborne remote sensing.

**Qiaozhi Hua** received the M.E. and Ph.D. degrees from the Graduate School of Global Information and Telecommunication Studies, School of Fundamental Science and Engineering, Waseda University, Tokyo, Japan, in 2015 and 2019, respectively. He is currently a Lecturer with the Computer School, Hubei University of Arts and Science, Xiangyang, China. His research interests include information-centric networking, the Internet of Things, artificial intelligence, C-V2X, edge computing, and information securityreceived the B.S. degree from Shenyang Ligong University, shenyang, China, in 2011, and the M.S. degree from University of Electronic Science and Technology of China, Chengdu, China, in 2015. She was a software engineer in the Tencent Technology (Shenzhen) Co., Ltd and ZTE Corporation, China, from 2016 to 2020. Since 2020, she is a design and development engineer with the Beijing Research Institute of Telemetry, China. Her research interests include architecture and protocol design of wireless networks.

**Osama Alfarraj** received the master's and Ph.D. degrees in information and communication technology from Griffith University, in 2008 and 2013, respectively. He is currently a Professor of computer sciences with King Saudi University, Riyadh, Saudi Arabia. His current research interests include eSystems (eGov, eHealth, and ecommerce), cloud computing, and big data. For two years, he has served as a Consultant and a member for the Saudi National Team for Measuring E-Government, Saudi Arabia.

**Jiankang Zhang** received the B.S. degree in mathematics and applied mathematics from Beijing University of Posts and Telecommunications, Beijing, China, in 2006, and the Ph.D. degree in communication and information systems from Zhengzhou University, Zhengzhou, China, in 2012. He is a Senior Lecturer with Bournemouth University, Poole, U.K. Prior to joining in Bournemouth University, he was a Senior Research Fellow with the University of Southampton, Southampton, U.K. He was a Lecturer from 2012 to 2013 and then an Associate Professor from 2013 to 2014 with Zhengzhou University, Zhengzhou, China. His research interests are in the areas of aeronautical communications and networks, evolutionary algorithms, machine learning algorithms, and edge computing. Dr. Zhang serves as an Associate Editor for IEEE ACCESS.